

Plasmonic Optical Tweezers for Particle

Manipulation: Principles, Methods, and Applications

Yatao Ren^{1,2}, Qin Chen¹, Mingjian He², Xiangzhi Zhang³, Hong Qi², and Yuying Yan^{,1,3}*

1 Faculty of Engineering, University of Nottingham, University Park, Nottingham NG7 2RD, UK

2 School of Energy Science and Engineering, Harbin Institute of Technology, Harbin 150001,

P.R. China

3 Research Centre for Fluids and Thermal Engineering, University of Nottingham, Ningbo

China, Ningbo 315100, P.R. China

ABSTRACT: Inspired by the idea of combining conventional optical tweezers with plasmonic nanostructures, a technique named plasmonic optical tweezers (POT) has been widely explored from fundamental principles to applications. With the ability to break the diffraction barrier and enhancing localized electromagnetic field, POT techniques are especially effective for high spatial-resolution manipulation of nanoscale or even sub-nanoscale objects, from small bioparticles to atoms. In addition, POT can be easily integrated with other techniques such as lab-on-chip devices which results in a very promising alternative technique for high-throughput single bioparticle sensing or imaging. Despite its label-free, high-precision, and high-spatial-resolution nature, it also suffers from some limitations. One of the main obstacles is that the plasmonic nanostructures are located over the surfaces of a substrate, which makes the manipulation of bioparticles turns from a 3D problem to a nearly 2D problem. Meanwhile, the operation zone is limited to a pre-defined area. Therefore, the target objects must be delivered to the operation zone near the plasmonic structures. This review summarizes the state-of-the-art target delivery methods

for the POT-based particle manipulating techniques, along with its applications in single-bioparticle analysis/imaging, high-throughput bioparticle purifying, and single-atom manipulation. Besides, future developmental perspectives of POT techniques are also discussed.

KEYWORDS: plasmonic optical tweezers; optofluidic; optical trapping and sorting; optical force; lab-on-a-chip; delivery methods; near-field interaction; electromagnetic enhancement; plasmonic resonance; nanoparticles

Manipulation of micro- or nano-objects, such as plasmonic nanoparticles, biological cells, or viruses, is of significant importance for biomedical or physical applications, such as micro-/nano-fabrication,¹⁻³ particle and/or cell sorting,⁴⁻⁶ single-cell analysis,⁷⁻¹⁰ or even single molecular and atom level operations.¹¹⁻¹⁵ In the past few decades, different methods have been proposed and developed to meet all kinds of application scenarios, including electrokinetic,^{16, 17} magnetic,¹⁸⁻²⁰ hydrodynamic,^{21, 22} and optical²³⁻²⁵ forces. Particularly, optical tweezer is one of the most promising techniques that can be used for the manipulation of micro- or nano-objects, for which Arthur Ashkin has been awarded the Nobel Prize of physics in 2018.

The conventional concept of optical tweezers was proposed in the 1970s.^{26, 27} It is based on a simple fact that light also has linear momentum which can be transferred to the interacting objects.²⁸ This momentum exchange is responsible for gradient and scattering forces. By carefully tuning the intensity and geometrical parameters of the focused incident light, the irradiated small particles can be trapped or manipulated. However, the spatial resolution of conventional optical tweezer is subject to the diffraction limit, which seriously restricts the applications of optical tweezers for nano-scale objects.²⁹⁻³¹ Besides, the optical forces acting on a sphere are proportional to the third power of the particle radius.²⁹ It means that with the reduction in particle size, the high-intensity laser should be used to enhance the optical forces, which may damage the bioparticles

and induce serious thermal effects. Moreover, it is extremely difficult to detect the trapping or sorting process of small nanoparticles through conventional fluorescence imaging methods.³² Therefore, the so-called plasmonic optical tweezer (POT) is proposed to break through this limitation, while improving the scale of optical force and depth of the potential well. This is achieved by enhancing the gradient and strength of the local electromagnetic field with the assistance of plasmonic structures.^{29, 33} Moreover, it can also be employed in the field of high-resolution and high-throughput manipulation and characterization of micro- and nano-particles at moderate laser powers.^{34, 35} The basic principle of POT is to combine the idea of nanoplasmonics and optical tweezers.²⁸ Therefore, nanofilm, array of nanocavities, isolated plasmonic micro- or nano-particles or plasmon antennas or other structures are usually involved,^{36, 37} which are easy to fabricate due to the rapid development of nanofabrication techniques.^{38, 39}

In the applications of POT techniques, the movement of particles or cells is partially induced by well-controlled forces, for example, the optical force, which is loaded on the targets. They are also exposed to other external forces, such as the drag force of fluid and Brownian force, which make it even harder to control or trap the targets. For optical force induced particle sorting or trapping, most of the recent studies are focused on the manipulating of particles in a stagnant or slowly moving fluid environment,^{33, 37, 40} which basically means that the optical force only needs to be sufficiently high to suppress the Brownian motion. However, the fluid-flow-induced particle movement or the active particle motion (not induced by fluid drag force), which is essential for the delivery of target objects to the trapping spot, also needs to be considered for the applications of high-throughput sorting or analyzing of particles or cells. Naturally, the optical force needed for trapping or sorting target objects will increase along with the increase of the fluid or particle velocity. Although this force can be further improved by increasing the laser power, the

accompanying side effects, such as localized heating, bubble formation, enhancement of Brownian motion, and thermophoresis will reduce the applicability of this technique.⁴⁰⁻⁴² It is found that this is achievable if the manipulation speed is lower than 0.15 $\mu\text{m/s}$ (for gold or silver nanospheres with diameter 100 nm) or 0.17 $\mu\text{m/s}$ (for polystyrene sphere with diameter 160 nm) for conventional optical tweezers. As a contrast, for dielectric particles larger than 1000 nm, the manipulation speed can be higher than 225 $\mu\text{m/s}$ (see Figure 1a).⁴⁰ Furthermore, this limitation can be surpassed with the assistance of plasmonic enhancement of local electromagnetic field. Therefore, by integrating with lab-on-chip applications and plasmon-enhanced sensing techniques, the POT techniques are very promising to be applied in the applications, such as high-throughput bioparticles detection, analysis, and sorting. Figure 1b shows an example of an integrated particle trapping and sorting system based on POT and lab-on-chip devices. Particles flow through the micro-channel at a controllable speed. At the bottom of the micro-channel, various configurations of plasmonic structures can be fabricated in the trapping region or sorting region. When irradiated by laser in the trapping region, the generated optical force and electromagnetic enhancement are responsible for trapping and corresponding sensing, imaging, or analyzing of the trapped particles such as surface-enhanced Raman scattering of a single molecule. Afterward, the particles are released to the sorting region, where the size- or component-dependent optical forces are utilized to push or drag the target particles to different channels.

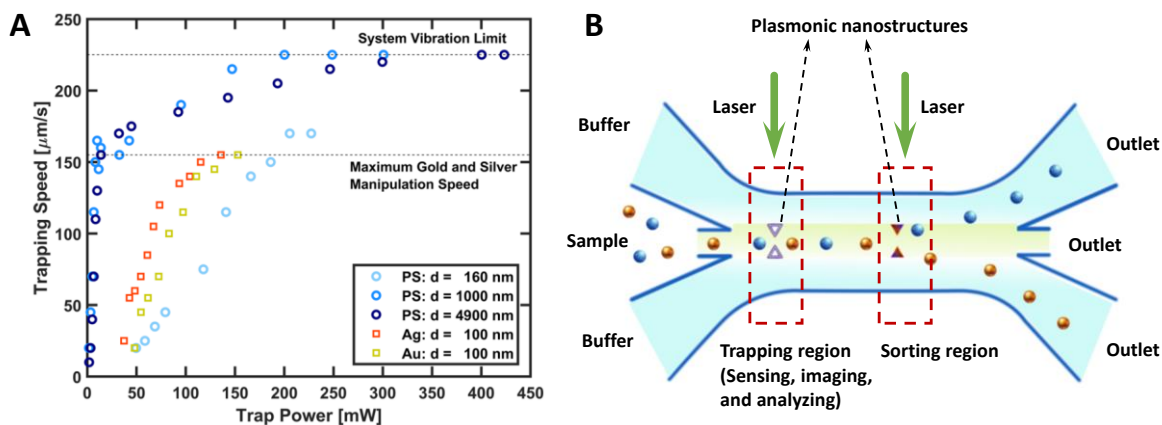


Figure 1. Limitation and application of optical tweezer on particle manipulation. (A) Limitation of optical tweezer nanoparticle manipulation speeds. Reprinted with permission from ref 40. Copyright 2018 American Chemical Society. (B) POT integrated lab-on-chip application for particle detection, analysis, and sorting.

Recently, the fundamentals and progress of the plasmonic optical tweezers techniques are reviewed.^{29, 33, 43, 44} Their main focus is the development of different plasmonic nanostructures and mechanisms for the application of particle trapping in a closed container or cavity, like a microchamber, where the target particles are delivered to the optical tweezer *via* diffusion effect. As far as we know, no one has systematically reviewed the high-efficiency delivery methods for particle manipulations in a flow environment (both fluid and particle motion). For most POT techniques, it is crucial to develop high-throughput lab-on-chip applications since the manipulation spots are located in a very limited and pre-defined area and the diffusion process is relatively time-consuming. Therefore, in this review, we mainly focus on the delivery methods or dynamic manipulation of moving target particles to the operation zone of plasmonic optical tweezers, followed by the corresponding applications and prospects. We first introduce the basic mechanism of particle manipulation based on optical force with plasmonic enhancement. Afterward, the commonly used configuration and materials for localized electromagnetic enhancement are

summarized, and then the delivery methods of POT-based particle manipulation techniques are reviewed. The potential applications of POT integrated lab-on-chip devices are also introduced briefly. Finally, the current challenges and perspectives are provided.

BASIC PRINCIPLE OF MICRO-/NANO-SCALE OBJECT MANIPULATION BY LIGHT

In order to manipulate micro- or nano-particles in fluid, we need to know precisely the forces that act on particles, both volume and surface forces, such as hydrodynamic and optical forces. In the case of optofluidics, the motion of a particle can be determined by the following equation:

$$m_0 \frac{d^2 \mathbf{r}}{dt^2} = \mathbf{F}_{\text{drag}} + \mathbf{F}_{\text{opt}} + \mathbf{F}_{\text{g}} + \mathbf{F}_{\text{B}} + \mathbf{F}_{\text{other}} \quad (1)$$

where m_0 is the mass of the particle. \mathbf{F}_{drag} , \mathbf{F}_{opt} , \mathbf{F}_{g} , \mathbf{F}_{B} , and $\mathbf{F}_{\text{other}}$ are the fluid drag force, optical force, gravity force with buoyancy, Brownian force, and other forces. The other forces denote the external forces including, but not limited to, electrical, electrokinetic, magnetic, optoelectronic, electrostatic, and thermophoresis forces,⁴⁴ which may be added to achieve additional control of the particles.

Optical Force. The optical forces acting on micro- or nano-particles are induced by the momentum exchange between photons and irradiated particles. Generally, these forces can be divided into gradient force and scattering force (or radiation pressure).⁴⁵ These forces can be separately calculated or summarized by the Maxwell stress tensor (\mathbf{T}).⁴⁶ The particles will be pushed forward by the scattering force along the light propagation direction (axial direction), while the gradient force will point toward the position of highest light intensity. Therefore, to enhance the optical force, one can either improve the laser intensity or the light field gradient. When the size of a particle is much larger than the incident wavelength, then the optical force can be calculated from the ray optics. Figure 2 illustrates the optical forces acting on an isolated Mie particle irradiated by a focused and collimated laser beam. For a focused laser beam, both gradient force and

scattering force will act on the particles. However, for a collimated beam, there is only scattering force owing to the lack of light field gradient. It means that focused laser should be applied to trap an object, which is also one of the drawbacks of traditional optical tweezers. Apparently, for a focused beam, the trapping position for a particle is located in the beam waist on the condition that the gradient force is much larger than the scattering force. However, when the size of a particle is much smaller than the incident wavelength, the particle can be regarded as a dipole, where Rayleigh approximation is applicable.⁴⁷ On the other hand, when the size of a particle is comparable to the incident wavelength, the electromagnetic theory must be fully considered to solve the Maxwell's equations.

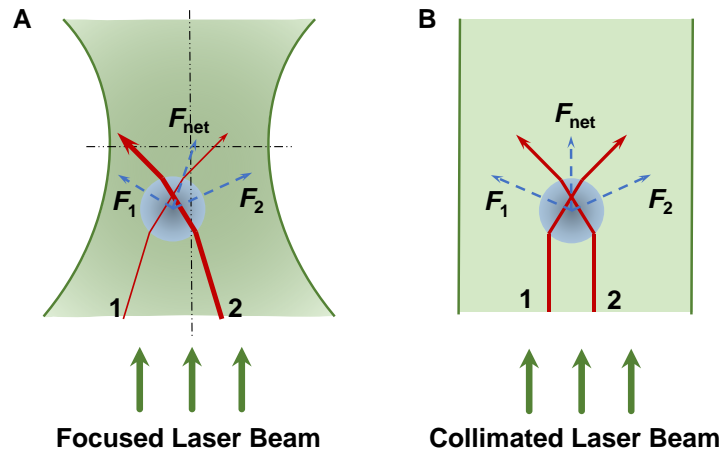


Figure 2. Schematic of an isolated Mie particle under irradiation of (A) focused laser beam and (B) collimated laser beam.

Compared to the traditional optical tweezers, the optical forces acting on the particles become far more complicated by inclusion of plasmon enhancement. In this situation, the optical forces can be obtained by integrating the above-mentioned Maxwell stress tensor around the target surface, which can be expressed as follows:⁴⁸

$$\mathbf{T} = \left[\varepsilon\varepsilon_0\mathbf{E}\mathbf{E} + \mu\mu_0\mathbf{H}\mathbf{H} - \frac{1}{2}(\varepsilon\varepsilon_0|\mathbf{E}|^2 + \mu\mu_0|\mathbf{H}|^2)\mathbf{I} \right] \quad (2)$$

where ε_0 and μ_0 denote the dielectric constant and magnetic susceptibility of the target object, respectively. ε and μ are the dielectric constant and magnetic susceptibility of the surrounding matrix media. \mathbf{I} represents the identity tensor.

For harmonic electromagnetic fields, the time-averaged Maxwell stress tensor can be expressed as:^{49, 50}

$$\langle \mathbf{T} \rangle = \frac{1}{2} \text{Re} \left[\varepsilon \varepsilon_0 \mathbf{E} \mathbf{E}^* + \mu \mu_0 \mathbf{H} \mathbf{H}^* - \frac{1}{2} (\varepsilon \varepsilon_0 \mathbf{E} \mathbf{E}^* + \mu \mu_0 \mathbf{H} \mathbf{H}^*) \mathbf{I} \right] \quad (3)$$

Hence, the optical force of an object in electromagnetic field can be written as:^{49, 50}

$$\mathbf{F}_{\text{opt}} = \oint \langle \mathbf{T} \rangle \cdot \mathbf{n} dS \quad (4)$$

where \mathbf{n} is the unit normal vector to the particle surface. Then the trapping potential energy for a particle located at r_0 can be obtained as follows:^{37, 51}

$$U(r_0) = \int_{\infty}^{r_0} \mathbf{F}_{\text{opt}}(r) \cdot dr \quad (5)$$

This is a very important figure of merit to define the stability of an optical trap which has been used in numerous investigations.⁵²⁻⁵⁴ When other forces are not considered, the depth of the potential well should satisfy $\exp(-U/k_B T) \ll 1$ (normally $U > 10k_B T$ is applied³⁷) to suppress the Brownian motion of a particle.⁵⁵

Contrast to traditional optical tweezers, the optical forces of POT are induced by incident light and scattering light, which is significantly enhanced by the plasmonic nanostructures. Therefore, the electromagnetic field cannot be easily defined by adjusting the incident laser. Consequently, the simulation of optical force is relatively complicated due to its dependency on external factors, such as configuration, size, and material of the nanostructures, in addition to the energy distribution of the laser beam. The Maxwell's equations need to be solved to obtain the 3D electromagnetic field which considers the light-matter interaction. Afterward, the optical force can

be determined by Maxwell stress tensor as illustrated in Eqs. (2-4). Different methods have been proposed to solve the light-matter interaction problems in the time domain or frequency domain, which will be introduced later.

Drag Forces Induced by Fluid flow. The fluid flow in lab-on-chip applications always falls into the laminar flow regime. Therefore, the drag force acting on the particles can be calculated based on the Stokes' law, which can be expressed as:⁴⁰

$$\mathbf{F}_{\text{drag}} = 6\pi\eta a\mathbf{v} \quad (6)$$

where η is the dynamic viscosity of the fluid. a is the radius of the target particles or cells. \mathbf{v} is the relative speed of the targets compared to the fluid. Generally, the drag force can be triggered by two reasons: the motion of fluid or the motion of the target particle. Basically, the former one can be induced by pressure or thermal gradient. Even if the fluid is stagnant, the motion of the target particles can also induce fluid drag force. This can be actuated by many external driving forces, such as the above-mentioned optical force, electrical field force, magnetic field force, or thermophoresis force.

Generally, the light-nanostructure interaction will lead to temperature rise of the plasmonic structures and the surrounding media. This thermal effect and accompanying thermal gradient may induce the convection of surrounding fluid (natural convection or Marangoni convection).^{56, 57} For natural convection, the velocity field can be obtained by solving the coupled energy and momentum equations:⁵⁸

$$\begin{cases} \rho_p c_p \partial_t T(\mathbf{r}, t) - k_p \nabla^2 T(\mathbf{r}, t) = q(\mathbf{r}), & \text{inside plasmonic structures} \\ \rho_f c_f [\partial_t T(\mathbf{r}, t) + \nabla \cdot (T(\mathbf{r}, t) \mathbf{v}(\mathbf{r}, t))] - k_f \nabla^2 T(\mathbf{r}, t) = 0, & \text{outside plasmonic structures} \end{cases} \quad (7)$$

$$\partial_t \mathbf{v}(\mathbf{r}, t) + (\mathbf{v}(\mathbf{r}, t) \cdot \nabla) \mathbf{v}(\mathbf{r}, t) = \nu \nabla^2 \mathbf{v}(\mathbf{r}, t) + \mathbf{f}(T(\mathbf{r}, t)) \quad (8)$$

where ρ , c , and k represent the mass density, specific heat, and thermal conductivity, respectively. The subscripts “p” and “f” denote properties of plasmonic structures and working fluid, respectively. T represents the temperature of plasmonic structure and fluid. ν is the dynamic viscosity of working fluid. q denotes the heat source inside the nanostructure induced by light-matter interaction:⁵⁸

$$q(\mathbf{r}) = \frac{\omega}{2} \text{Im}(\varepsilon) |\mathbf{E}(\mathbf{r})|^2 \quad (9)$$

where ω is the angular frequency of incident light. \mathbf{f}_{th} represents the buoyancy force induced by the temperature-dependent mass density of surrounding working fluid, which can be expressed as:⁵⁸

$$\mathbf{f}_{\text{th}}(T) = \beta g \delta T(\mathbf{r}, t) \mathbf{u}_z \quad (10)$$

where δT is the temperature increase. β is the dilatation coefficient of the working fluid. g is the gravitational acceleration and \mathbf{u}_z is the upward unit vector. Then, the velocity field can be obtained, which can be used to calculate the drag force acting on the target particles.

The Marangoni flow refers to the fluid flow along the interface of two fluids (typically liquid and air) caused by the surface tension gradient. Generally, the surface tension is a temperature-dependent factor. Hence, thermal gradient along the fluid interface can also induce Marangoni flow, which is also known as thermal-Marangoni flow.⁵⁹ Regarding POT, the thermal gradient is generated by the plasmonic heating effect. The thermal-Marangoni convection flow is found to be much stronger than natural convection.⁶⁰ The driving force along the interface is proportional inversely to the thermal gradient, which can be expressed as:⁵⁷

$$\tau_s = -\sigma_T \nabla T \quad (11)$$

where σ_T denotes the temperature coefficient of surface tension.

Brownian Force and Thermophoresis. The Brownian force refers to the integrated forces around the surface of a particle, which is induced from the momentum exchange between the surrounding particles and molecules. It will result in the random movement of a particle emerged in a gas or liquid environment, which is known as the Brownian motion. In order to explain this random motion, numerous models have been proposed with the help of statistical mechanics theories, such as Einstein's theory and Smoluchowski model.⁶¹ However, a much easier way to solve this is using the Newtonian framework, where the Brownian motion of a particle is regarded as the results of a continuous and random force acting on the particle, which can be expressed as:^{61, 62}

$$\mathbf{F}_B = \mathbf{R}_{\text{random}} \sqrt{\frac{12\pi k_B T r \eta}{\Delta t}} \quad (12)$$

where $\mathbf{R}_{\text{random}}$ is a random vector with Gaussian random number components between 0 and 1 of zero mean. k_B and T are the Boltzmann constant and absolute temperature, respectively. r represents the radius of the particle. Afterward, the Brownian motion of a particle can be determined by Newton's law of motion.

Similar to the Brownian force, the thermophoretic force acting on the target particles is also induced by the momentum exchange between the surrounding particles and molecules. The Brownian force is a random force, however, the thermophoretic force is related to the temperature gradient in the solutions. Due to the higher momentum of hot molecules, the momentum exchange at the hot side of the particle is larger compared to the cold side. Hence, the target particles will be pushed by the thermophoretic force to move to the cold side, which can be expressed as:⁶³

$$\mathbf{F}_T = -\alpha_T k_B \nabla T \quad (13)$$

where α_T is the thermal diffusion coefficient of the target particle, which can be calculated by:⁶³

$$\alpha_T = S_T T \quad (14)$$

where $S_T = D_T/D$ is the Soret coefficient. D and D_T are the Brownian and thermal diffusion coefficients, respectively.⁵⁷

Other Forces. Except for the above-mentioned forces, the particles may be also driven by other forces, such as electrokinetic, magnetic, optoelectronic, and electrostatic forces,^{44, 64, 65} depending on the specific mechanism and configuration of the manipulation devices. The details of these forces have been reviewed in Ref. 66, which will not be repeated here.

Localized Electromagnetic Field Enhancement of Plasmonic Structures. One of the most essential issues in the development of POT is the localized enhancement of electromagnetic field intensity and gradient. There are two typical types of surface plasmons that are known to be helpful for the manipulation of particles, *i.e.* surface plasmon polaritons (SPPs) and localized surface plasmon (LSPs).⁶⁷ The main difference between these two surface plasmons is the dimension of the plasmonic materials. SPPs sustains at flat and extended metal interfaces, while LSPs exist in nanopores or nanoparticles which are in the subwavelength scale.⁶⁷ Generally, the LSPs are frequently used to assist the optical manipulation and other applications due to their excellent performance of nanostructures in the enhancement of the local electromagnetic field. As a result, the plasmonic enhancement of different kinds of materials, morphologies, and configurations has been investigated. It is proposed that the Farady number can be used to quantify the ability of this enhancement of plasmonic sphere, which takes the properties of the surrounding media into consideration and can be calculated without numerical simulations:⁶⁸

$$Fa = |E_{\max} / E_0|^2 = 9 \left| \frac{\epsilon}{\epsilon + 2\epsilon_s} \right| \quad (15)$$

where ϵ_s is the dielectric permittivity of the surrounding dielectric media. It is apparent that the Faraday number is applicable for different materials, such as nanoparticles and matrix media,

illuminated by different wavelengths. However, this figure of merit is only applicable to isolated nanospheres. Till now, no general rules or principles are available to compare the efficiency of complex geometries or configurations, such as nanoantenna or nanopore. The reason behind this is the near-field interaction. Therefore, the actual enhancement ability of a specific configuration can be evaluated from analytical, numerical, or experimental methods.

Analytical solutions like Mie solutions or T-matrix method are very popular for the calculation of electromagnetic fields of light-matter interaction. Unfortunately, they are basically more suitable for relatively simple geometries, and cannot be applied for the situations where the plasmonic structures are located at the interface of two media, which is always the situation for POT.⁶⁹ Therefore, numerical methods are widely used to predict the electromagnetic field and optical forces of particles, located near plasmonic structures. Basically, these numerical methods can be classified into two categories, time-domain and frequency-domain methods.⁷⁰ For both of these methods, Maxwell's equations need to be solved:^{69, 71}

$$\nabla \times \mathbf{E} = -\frac{\partial \mathbf{B}}{\partial t} \quad (16)$$

$$\nabla \times \mathbf{H} = \frac{\partial \mathbf{D}}{\partial t} + \mathbf{J} \quad (17)$$

$$\nabla \cdot \mathbf{E} = \frac{1}{\varepsilon} \rho \quad (18)$$

$$\nabla \cdot \mathbf{B} = 0 \quad (19)$$

For homogeneous and isotropic media, optical properties like dielectric functions ε , permeability μ , and conductivity σ can be written as a scalar form. By using the linear constitutive relations:⁶⁹

$$\begin{cases} \mathbf{J} = \sigma \mathbf{E} \\ \mathbf{D} = \varepsilon \mathbf{E} \\ \mathbf{B} = \mu \mathbf{H} \end{cases} \quad (20)$$

Hence, Eqs. (16-17) can be expressed as:

$$\nabla \times \mathbf{E} = -\mu \frac{\partial \mathbf{H}}{\partial t} \quad (21)$$

$$\nabla \times \mathbf{H} = \sigma \mathbf{E} + \varepsilon \frac{\partial \mathbf{E}}{\partial t} \quad (22)$$

For time-domain methods, Eqs. (16-17) are equivalent to the following scalar equations:⁷²

$$\left\{ \begin{array}{l} -\frac{\partial B_x}{\partial t} = \frac{\partial E_z}{\partial y} - \frac{\partial E_y}{\partial z} \\ -\frac{\partial B_y}{\partial t} = \frac{\partial E_x}{\partial z} - \frac{\partial E_z}{\partial x} \\ -\frac{\partial B_z}{\partial t} = \frac{\partial E_y}{\partial x} - \frac{\partial E_x}{\partial y} \\ \frac{\partial D_x}{\partial t} + J_x = \frac{\partial H_z}{\partial y} - \frac{\partial H_y}{\partial z} \\ \frac{\partial D_y}{\partial t} + J_y = \frac{\partial H_x}{\partial z} - \frac{\partial H_z}{\partial x} \\ \frac{\partial D_z}{\partial t} + J_z = \frac{\partial H_y}{\partial x} - \frac{\partial H_x}{\partial y} \end{array} \right. \quad (23)$$

Then the above equations can be solved by various techniques such as the finite-difference time-domain method.⁷² As for frequency-domain methods, the incident light can be regarded as a plane wave with frequency ω . Then the time-harmonic or frequency-domain form Maxwell's equations can be written as:⁶⁹

$$\nabla \times \mathbf{E} = i\omega\mu\mathbf{H} \quad (24)$$

$$\nabla \times \mathbf{H} = (\sigma + i\omega\varepsilon)\mathbf{E} \quad (25)$$

Then we can obtain:⁶⁹

$$\frac{1}{\mu}(\nabla \times \nabla \times \mathbf{E}) - (\omega^2 \varepsilon - i\omega\sigma)\mathbf{E} = 0 \quad (26)$$

Different numerical methods have been proposed to solve the above-mentioned time-domain or frequency-domain equations, among which, the most commonly used numerical methods include finite element method, finite-difference time-domain method, boundary element method, discrete dipole approximation, T matrix method, *etc.* These can be executed using commercial software, such as Comsol Multiphysics and Lumerical, or open-source code like DDSCAT and MNPBEM.⁷³⁻⁷⁷ Due to the convenience of numerical simulations, the simulated results are often used as a guide for the geometry design or material selection for the plasmonic structures. In the case of an experimental approach, the localized electromagnetic field is extremely hard to directly detect or observe. Usually, it is characterized by indirect phenomena or by-products like Raman signal enhancement, fluorescence intensity, surface potential, *etc.*⁷⁸⁻⁸⁰

CONFIGURATIONS OF PLASMONIC STRUCTURES AND MATERIALS

Owing to the excellent performance of plasmonic structures, such as high enhancement ability, ease to fabricate (*vide supra*), they are widely used to enhance the local electromagnetic field in the applications of optical-tweezer-based microfluidics, including different kinds of materials and structures. Figure 3 illustrates some typical configurations of plasmonic structures applied in the POT technique, including nanorod, nano-bowtie, nanodimer, *etc.* Basically, they can be roughly characterized into four categories: a) isolated plasmonic structures; b) plasmonic nanostructure with near-field interaction; c) nanocavity in plasmonic nanofilm; d) other kinds of configurations. It should be clarified that for most cases the nanostructures appear in the form of arrays,⁴⁴ even if they are classified as isolated plasmonic structure or nanocavity, as long as the near-field interaction can be neglected due to the sufficient interparticle distance. To further illustrate the characteristics of each category, the corresponding electric field enhancement ability and optical

force for different plasmonic structures utilized in POT in recent literature are summarized in Table 1. It can be analyzed from Table 1 that although many different types of materials like chromium, nickel, palladium, titanium, metal nitrides, *etc.*, are investigated in the field of nanoplasmonics,^{68, 81} gold nanostructures are still the most popular choice in the application of plasmonic optical tweezers related studies. This may be due to its well-established fabrication techniques. Furthermore, the sizes of the plasmonic structures are ranging from tens of nanometers to a few micrometers. Considering the fact that the hotspot is smaller than the plasmonic structures, the spatial resolution can be improved to nanometer scale.

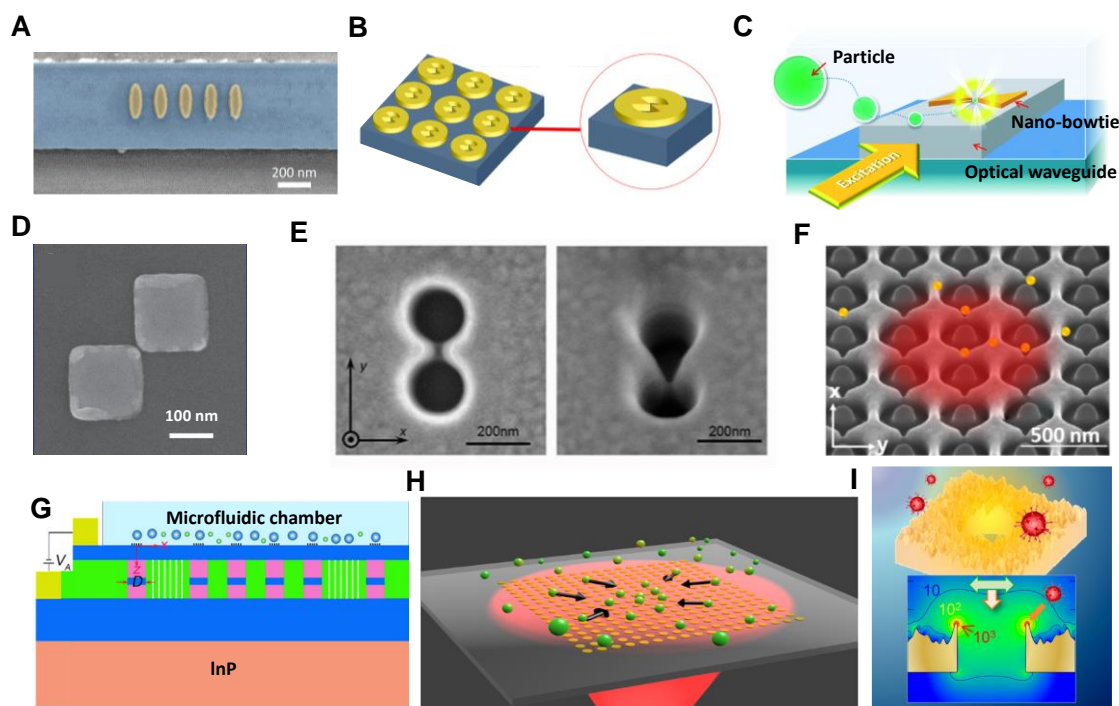


Figure 3. Typical configuration of plasmonic structures in POT. (A) Nanorod. Adapted with permission from ref 82. Copyright 2020 American Chemical Society. (B) Nano-bowtie ring tweezer. Adapted with permission from ref 83. Copyright 2019 Elsevier (C) Nano-bowtie. Adapted with permission from ref 84. Copyright 2014 Royal Society of Chemistry (D) Nanoblock dimer. Adapted with permission from ref 85. Copyright 2013 American Chemical Society. (E) Double

nanohole apertures. Adapted with permission from ref 86. Copyright 2017 American Chemical Society. (F) Connected nanoring aperture. Adapted from ref 87, whose figures are licensed under Creative Commons Attribution License 4.0 (CC BY). (G) Graphene nanodot. Adapted with permission from ref 54. Copyright 2020 American Physical Society. (H) Plasmonic optical lattices. Reprinted with permission from ref 88. Copyright 2016 AIP Publishing. (I) Nanohole array with random nanospikes. Reprinted with permission from ref 89. Copyright 2017 American Chemical Society.

Table 1. Enhancement of local electric field by different configurations of plasmonic structures and materials

Category	Shapes	Materials	$\log E/E_0 ^2$	Optical force or stiffness	Scale	Simulation or experiment	More information
Isolated nanoparticles	Nanodisk	Au ⁹⁰	-	-	2 μ m	Simulation and experiment	Glass substrate
	Nanorod	Au ⁸²	-	<1.1 fN/nm	200 nm	Simulation and experiment	Silicon waveguide
	Nano-bowtie ring tweezer	Au ⁸³	-	~3.23 nN/W for a virion with radius 10 nm right above the structure	Hundreds of nanometers	Simulation	-
Nanoantenna	Nano-bowtie	Au ⁸⁴	-	~652 pN/W for polystyrene particles with 20 nm diameters	Hundreds of nanometers	Simulation and experiment	Waveguide and glass substrate
		Au ⁹¹	~3.0	-	-	Simulation	Fabricated on TiN thin film on glass or sapphire substrate
	Nanoblock dimer	Au	2.6 ⁸⁵	<2.5 fN/nm when laser power density equals 60kW/cm ²	Hundreds of nanometers	Simulation and experiment	Glass substrate
			3.8 ⁹²	-	-	Experiment	Glass substrate
	Nanorod dimer	Au ⁹³	7.5	-	Hundreds of nanometers	Simulation	Glass substrate
Graded nanorod	Au ⁹⁴	-	<600 pN/W for polystyrene particles with 40 nm diameters	Tens to hundreds of nanometers	Simulation	Fabricated on silicon waveguide and covered by silica	

Nanocavity or nanohole	Double nanohole apertures	Au ⁸⁶	<4.0	-	Hundreds of nanometers	Simulation and experiment	Glass substrate
		Au ⁹⁵	<2.4	<250 fN	Hundreds of nanometers	Simulation and experiment	Glass substrate
	Nanohole array ⁹⁶	Au	-	-	300 nm	Simulation and experiment	Combination of opto-thermo-electrohydrodynamic forces
Other configurations	Graphene nanodot ⁵⁴	Graphene	-	-	Tens of nanometers	Simulation	With quantum cascaded heterostructures as a built-in optical source
	Nano-ellipses metasurface ⁹⁷	Au	-	<1000pN/W/ μm^2	Hundreds of nanometers	Simulation	Silica substrate
	Slot-graphite photonic crystal ⁹⁸	Graphene	-	~80 pN/nm/W	-	Experiment	-
	Mobile nanotweezers ⁹⁹	Ag and Fe	-	-	A few micrometers	Experiment	Driven by magnetic field

Isolated Plasmonic Structures. Isolated plasmonic structures, including nanoarray without near-field interaction,^{83, 90} are commonly used to manipulate micro- and nano-particles in optical plasmonic tweezers. Different structures have been applied, which range from simple shapes, such as nanodisk,¹⁰⁰ nanowire,^{101, 102} and nanopillar¹⁰³ to complex configurations like nanodiabolo,¹⁰⁴ nano-bowtie ring,⁸³ and micro-cauldrons.¹⁰⁵ When illuminated by light of corresponding resonance wavelength, a strong field enhancement ($|\mathbf{E}/\mathbf{E}_0|^2$) is expected. In the case of silver nanorods, this enhancement could be as high as 3500.¹⁰⁶ However, for a small nanoparticle, the field enhancement decays with distance r from the particles as $1/r^3$.¹⁰⁷ On the other hands, this decay can be described as an expansion of multipolar modes of larger particles:^{108, 109}

$$E(r) = \frac{2\alpha E_0}{4\pi\epsilon_0 r^3} + \frac{3\beta E_0}{4\pi\epsilon_0 r^4} + \frac{4\gamma E_0}{4\pi\epsilon_0 r^5} + \dots \quad (27)$$

where α , β , γ are the dipole, quadrupole, octupole polarizability tensor, respectively. Therefore, the optical force, which is induced by field enhancement of plasmonic structures has a very limited effective zone. As a result, the target particles first need to be delivered to a location near the plasmonic optical tweezer to be trapped or sorted.

It is worth mentioning that for manipulating of plasmonic nanoparticles using traditional optical tweezers, the resonance enhancement is also very important, which should be fully exploited. There have been numerous studies focusing on the manipulation of plasmonic nanoparticles (especially Au and Ag) on- and off-resonance.^{3, 110-113} For on-resonance, which means the wavelength of the focused laser is matching with the localized surface plasmon resonance of the manipulated nanoparticles, the manipulation could provide higher precision using lower laser power compared to off-resonance conditions owing to the enhanced light-particle interaction.¹¹² Similarly, the manipulation precision of dielectric nanoparticles can be also improved through the magnetic dipolar resonance effect.¹¹⁴

Plasmonic Nanostructure with Near-Field Interaction. The near-field interaction is an efficient way to further enhance the local electromagnetic field compared to isolated plasmonic structures. When the plasmonic nanostructures are closely packed, the strongly confined electric field around each nanostructure will overlap and interact with one another.¹⁰⁸ Therefore, the local electric field can be further enhanced. This can be achieved by different kinds of nano- or micro-antenna (including dimers, trimers, tetramers),¹¹⁵⁻¹²⁰ and nanoarray.¹²¹⁻¹²³ Besides the configuration and size of the nano-assemblies, the field enhancement of plasmonic structures is strongly dependent on the polarization and wavelength of the incident light, and the gap distance between each other.^{107, 108, 124, 125} Figure 4 shows the field enhancement of nanosphere, nanorod, nanosphere dimer, and nanocavity. It can be seen that with near-field interaction, the field enhancement $|\mathbf{E}/\mathbf{E}_0|^2$ with near-field interaction could be a few or even hundreds of times larger than that of single nanoparticles for similar materials, shape, and size. Besides, for near-field interaction, the enhancement is also dependent on the gap distance or specific configuration. El-Sayed and co-workers have carried out a series of work to illustrate the plasmon coupling effect between nanoparticle aggregates.¹²⁶⁻¹²⁹ They found that the plasmon resonance coupling between nanoparticle dimers decays with the same trend for different particle sizes, shapes, and components. This provides the general guidelines for the selection of illumination wavelengths of POT. Furthermore, the field enhancement is typically confined in a small volume of a few to a few tens of nanometers around the light illuminated nanostructures (see Figure 4). Therefore, the development of this technique is severely limited by its inherent defect that the target particles need to be delivered to the predefined spots. In most of the present studies, the particles are delivered by the diffusion (thermal convection, thermophoresis, *etc.*) of the targets, which is extremely inefficient. To solve this problem, Jiang *et al.* reported a gold nano-ellipse array that

can realize 2D trapping and arbitrary-direction delivery of nanoparticles through the control of the polarization direction of linearly polarized light.⁹⁷ The orientations of the nano-ellipses are perpendicular to one another. Therefore, by altering the light polarization directions, the interaction patterns between the nano-ellipses will be changed, which consequently affects the distribution of 2D hotspots and potential wells. As a result, the target nanoparticles will be propelled by optical force to move from one potential well to another. This configuration could be beneficial for the expanding of the range of optical manipulation.

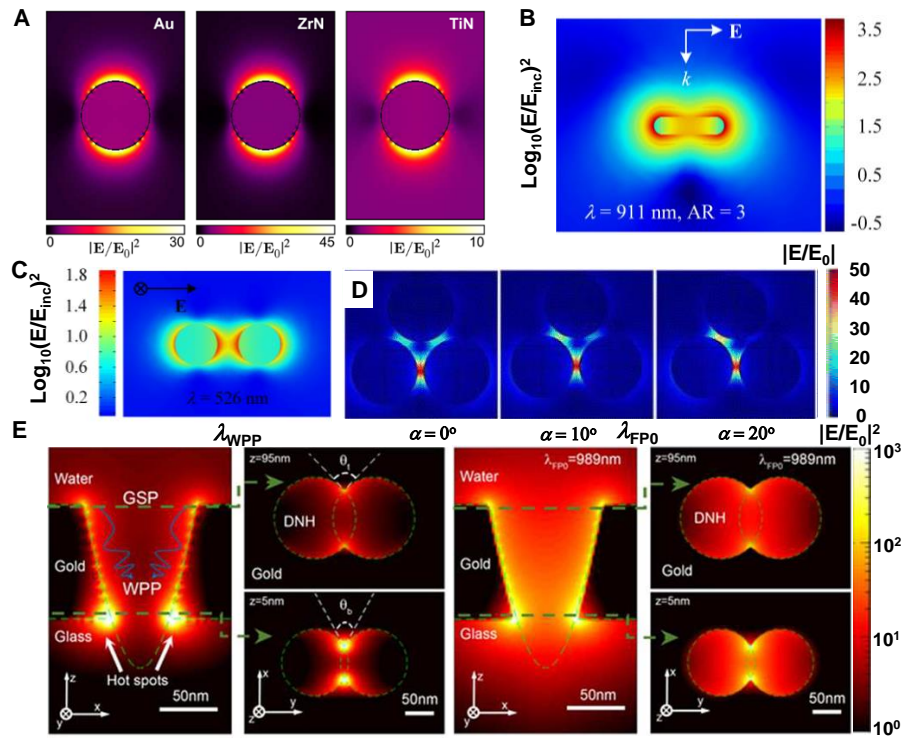


Figure 4. Field enhancement around light illuminated nanostructures. (A) Au, ZrN, and TiN nanosphere with 10 nm radius. Reprinted with permission from ref 68. Copyright 2015 American Chemical Society. (B) Au nanorod with effective radius 20 nm and aspect ratio 3. Adapted with permission from ref 130. Copyright 2018 Elsevier. (C) Au nanosphere dimer with radius 40 nm. Adapted with permission from ref 131. Copyright 2018 Elsevier. (D) Near-field interaction of nanosphere trimer. Adapted with permission from ref 132. Copyright 2015 Springer. (E) Au

nanocavity on a glass substrate. Adapted with permission from ref 86. Copyright 2017 American Chemical Society.

Nanocavity in Plasmonic Nanofilm. Compared to the technique of generating a strongly localized electromagnetic field based on plasmonic nanostructures on a substrate, the advantage of nanocavity or nanopore is to create a potential well at the hotspot between the nanocavity induced by the gap surface plasmon, which consequently enhances the local electromagnetic field.^{86, 133} For coaxial nanoapertures, multiple Fabry–Pérot resonances may also be easily excited.¹³⁴ Another advantage of using the nanocavity-based manipulation device is that the diffusion of the converted heat is relatively fast owing to the high thermal conductivity of the metallic substrates (typically gold),¹³⁴ and if the delivery efficiency of target particles is ignored, which will be discussed in the next section. Similar to nanostructures, the using of nanocavity to manipulate particles also can be achieved by single nanopore,¹³⁴ double nanopores,^{95, 135} or nanopore array.^{13, 136-138} Many studies have been carried out to investigate the effectiveness of using nanopore-based plasmon structures. Verschueren *et al.* achieved single protein manipulation using plasmonic nanopores enhanced optical tweezer.¹³⁵ The protein molecules are delivered by electrophoretic effect into the nanopore on a 100 nm/20 nm gold/silicon nitride film. This can be regarded as an inverted-bowtie aperture with ~60 nm side length, 140 nm width, and 20 nm gap width. The results show that the biomolecules can be confined around the nanopore with ~20-fold field enhancement (E/E_0) between the gap region. Xu *et al.* developed an optical trapping system based on double nanopore in a gold film with fluorescence microscopy, to directly track the position of target nanospheres.⁹⁵ Similarly, the trapping spot is also located in the gap region with about 14-fold enhancement of localized electric field. Comprehensive simulations are also performed to show the heat generation and corresponding fluid natural convection. Based on the double nanopore structures,

Ghorbanzadeh *et al.* used a conical shaped double nanopore apertures in a gold film to trap dielectric nanoparticles.⁸⁶ The results show that the aperture assisted optical trapping has very high sensitivity towards the size of dielectric nanoparticles, which is partly owing to 2D nanofocusing of coupled gap surface plasmon and wedge plasmon polaritons generated by the slope shape of the metallic wedges. Compared to the dozens of times field enhancement of regular nanopore structures, the enhancement of conical shaped double nanopore apertures can reach up to a hundred folds around the hotspots.

Other Configurations. Besides the above-mentioned configurations, there are many other ways to excite the surface plasmons, such as the built-in optical source based method,⁵⁴ mobile nanotweezers,⁹⁹ cylindrical bumps attached nanohole,¹³⁹ *etc.* Although, these methods are more complicated from the fabrication point of view, they can achieve multiple and complex functions in addition to trapping the targets. It is worth noticing that one of the advantages of POT compared to conventional optical tweezers is not requiring complex laser focusing equipment. The optical forces are induced by the confined electromagnetic field around the plasmonic structures. Therefore, the configuration of the entire POT-based technique can be further simplified by using a built-in optical source instead of an external laser.⁵⁴ Meanwhile, the conventional POT-based particles trapping, or sorting are limited by predefined spots where the plasmonic nanostructures are fabricated. To improve the moving speed of the target particles, Ghosh *et al.* proposed the concept of mobile nanotweezers to achieve the active manipulation of nano-objects.^{44, 99, 140, 141} This is very interesting as instead of localizing the strong electromagnetic field on a predefined hotspot located near substrates, they integrated the plasmonic nanostructures with the magnetically driven helical microrobots. Therefore, the microrobots can act as trapping points and delivery vehicles at the same time, which makes the delivery of the targets become selective and label-free.

This technique is promising for lab-on-chip applications and some intracellular environment as well.^{142, 143}

TRAPPING AND SORTING OF PARTICLES BY DIFFERENT DELIVERY METHODS

The delivery of targets plays an important role in the applications of POT techniques, mainly including particle trapping, sorting, and the following analyzing process. In this section, we reviewed the recent works concerning the manipulation of nano- or micro-particles (dielectric or plasmonic) or bioparticles with different delivery mechanisms that are divided into four categories: a) motion dominated by diffusion; b) motion induced by optical force; c) motion induced by fluid flow; d) motion of target particles induced by other external forces (see Figure 5). The first category has been systematically reviewed elsewhere.^{28, 29, 33, 37} Basically, in this category, the delivery of targets to the manipulating area is mainly depending on the diffusion or Brownian motion of the targets without any external assistance. So, this is a time-consuming approach for the diluted solutions of target particles. In this paper, we mainly focus on the last three categories. The frequently used delivery methods of POT and their limitations are summarized in Table 2. It can be seen that although the manipulation speed limitation for micro-/nano-scale particles is over a hundred micrometers per second.⁴⁰ In the present literature, the most commonly investigated trapping or sorting speed is in the range of a few micrometers per second to a few tens of micrometers per second. More importantly, the diffusion delivery method is frequently used for small-scale object manipulation, especially sub-10 nm objects. The reason behind this is the exponentially decreased optical force when reducing the particle sizes.²⁹

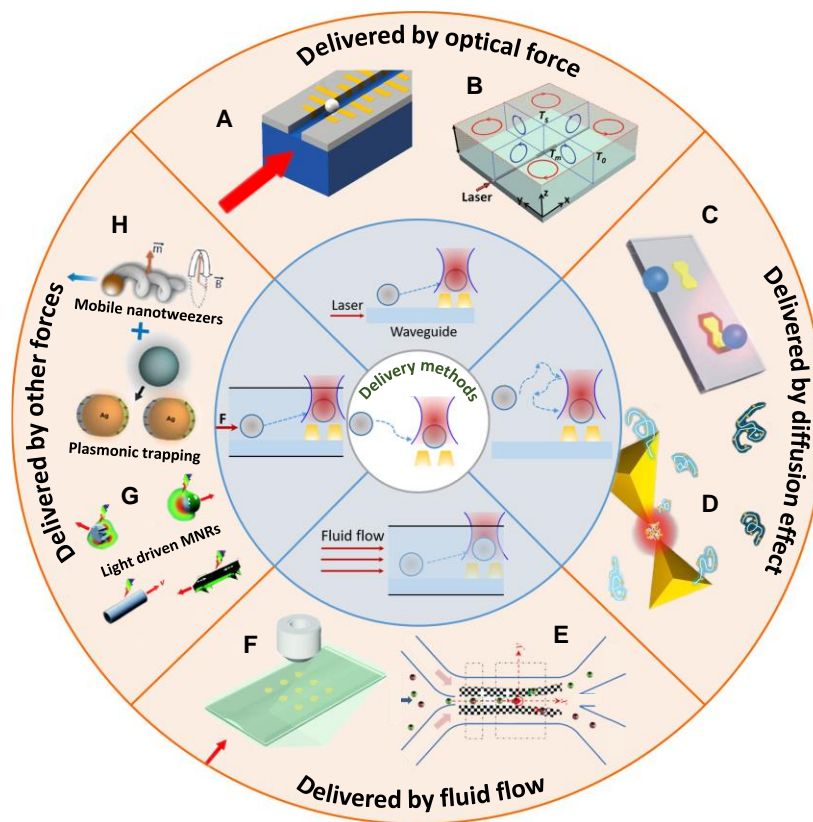


Figure 5. Delivery methods for plasmonic optical tweezing, including optical force induced delivery, diffusion dominated delivery, fluid flow induced delivery, and others. A Adapted with permission from ref 94, Copyright 2016 The Optical Society. B Adapted from ref 102, whose figures are licensed under Creative Commons Attribution License 4.0 (CC BY). C Adapted with permission from ref 104. Copyright 2011 Nature Publishing Group. D Adapted with permission from ref 144. Copyright 2012 American Chemical Society. E Adapted from ref 145, whose figures are licensed under Creative Commons Attribution License 4.0 (CC BY). F Adapted with permission from ref 90, Copyright 2009 The Optical Society. G Adapted from ref 146. Copyright 2017 Royal Society of Chemistry. H Adapted with permission from ref 99. Copyright 2018 American Association for the Advancement of Science.

Table 2. Typical delivery methods for POT applications and corresponding limitations.

Delivery method	Trapping or sorting	Target objects	size	Plasmon enhancing	Velocity	Refs.
(a) Diffusion	Trapping	Polystyrene sphere and bacteria	Polystyrene sphere: 200 nm Bacteria: 2x0.8 μm	Gold nanoantennas	-	118
	Trapping	Single proteins molecule	~ 6 nm	Coaxial nanoaperture	-	134
	Trapping	Polystyrene sphere and single protein molecule	10-20 nm	Plasmonic nanopores	-	135
(b) Optical force	Trapping	Polystyrene sphere	1 μm	Gold bowtie tweezers	Very slow	84
	Trapping	Yeast cells and polystyrene spheres	5-10 μm	Gold microdisks array	<4.5 $\mu\text{m/s}$	147
(c) Fluid flow	Trapping	Yeast cells and polystyrene spheres	Yeast cells: A few microns Polystyrene spheres: 2 and 3 μm	Gold microdisks array	Very slow	90
	Sorting	Dielectric bioparticles	0.1 to 1 μm	Plasmonic microlens	0.95 to 3 $\mu\text{m/s}$	148
	Sorting	Yeast cells	2 to 7 μm	None	20 to 60 $\mu\text{m/s}$	149
	Trapping and sorting	Dielectric particles	40 – 60 nm	Graphene Stripes	-	145
(d) Magnetic force	Trapping and sorting	Polystyrene sphere, silica sphere, and bacteria	Sub-micrometer to 2 μm	Mobile nanotweezers	~ 2 $\mu\text{m/s}$	99
(d) Electrothermoplasmonic flow	Trapping	Polystyrene sphere	300 nm	Gold nanodisks	<18 $\mu\text{m/s}$	150
(d) Electrothermoplasmonic flow and thermoplasmonic convection	Trapping	Polystyrene sphere	200 nm and 1 μm	Nanohole array on gold substrate	<30 $\mu\text{m/s}$	151

Motion Induced by Optical Force. Kawata *et al.* proposed a different optical manipulation method in 1992.¹⁵² Instead of using a focused laser beam to directly illuminate the target particle, they used the evanescent wave which results from the total reflection of a collimated laser beam, and to push forward the polymer microbeads.^{152, 153} Later, they further extended this method to be used in the surface of waveguide, where they successfully pushed a microscale latex particle to move at a speed of approximately 5 $\mu\text{m/s}$.¹⁵⁴ Particles located near the waveguide are exposed to scattering force that pushes the particle forward, and gradient force that limits the particles to the waveguide. Since then, this method has been further investigated and developed to be utilized in the field of particles trapping, sorting, and delivering.^{52, 53, 155-157} Schmidt *et al.* used the waveguide-based method to realize the dynamic trapping and delivery of particles in an integrated microfluidic/photonic architecture. It was demonstrated that the transport velocity is proportional to the laser power, and a maximum transport velocity of 28 $\mu\text{m/s}$ could be achieved (see Figure 6A).¹⁵⁸ In addition, without considering the fluid flow, Xu *et al.* proposed a multi-level sorting method using optical waveguide splitter, which demonstrates the flexibility of the waveguide-based method (see Figure 6B).⁵³ Similar to the optical force induced by directly focused laser irradiation, the evanescent wave also can be enhanced by the plasmonic structures that are integrated with the waveguide surface, which also can contribute to the trapping and sorting of micro-/nano-objects since usually the evanescent wave only leads to the delivering of the targets along the light path.¹⁴⁷ However, it should be noted that since this force is relatively small, the velocity of the particles remains at a low level, typically from a few tens of nanometers per second to a few tens of micrometers per second.^{147, 158-161} Therefore, the efficiency is limited due to the delivery speed of target objects into the trapping or sorting area. This maybe not applicable for the development of high-throughput lab-on-chip devices.^{99, 150} However, still, this method has some

advantages compared to conventional optical tweezer which is the substantially reduced light intensities.¹⁶²

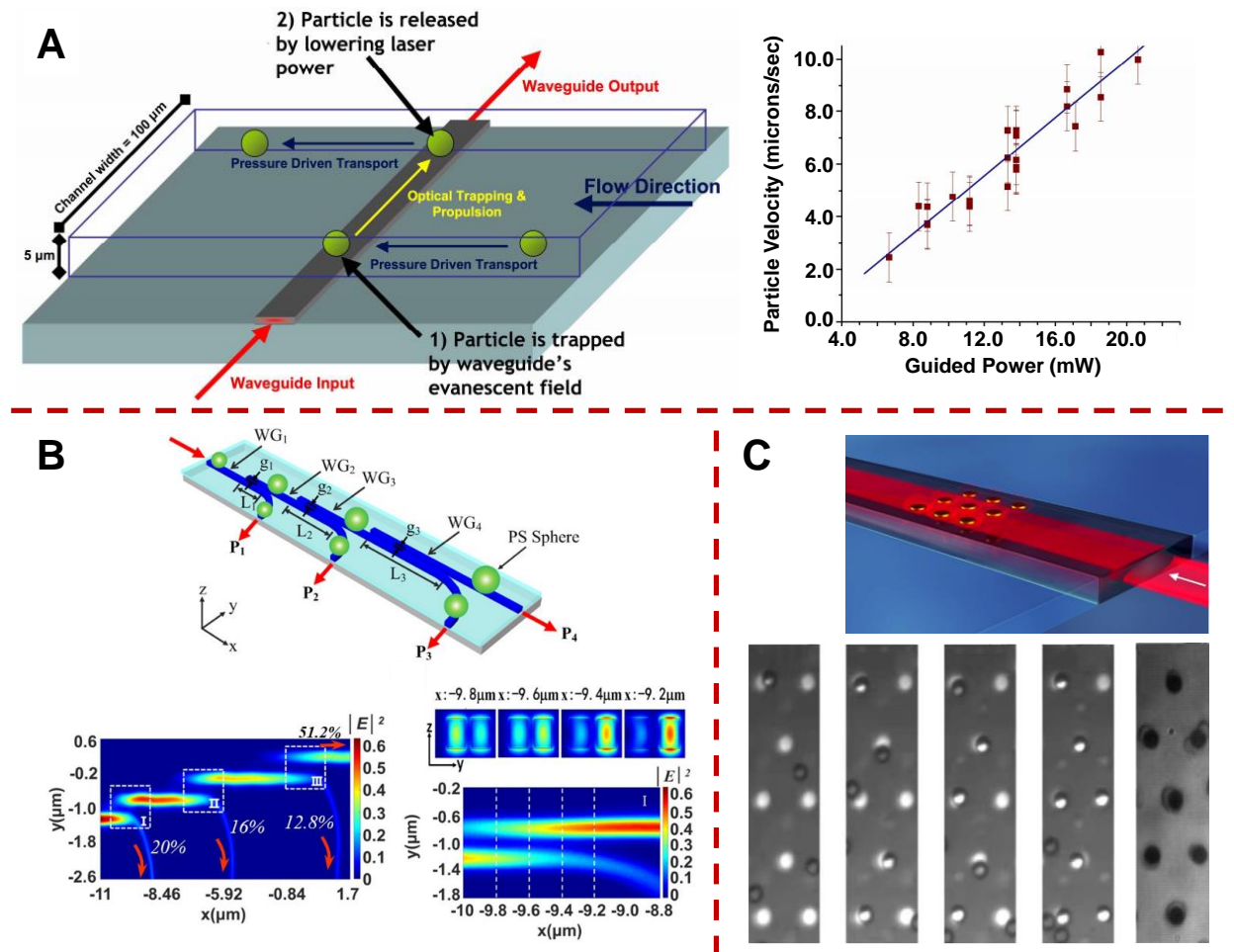


Figure 6. Particle delivering and manipulating based on waveguide. (A) Optical waveguide propulsion is perpendicular to the direction of the pressure driven flow. Adapted with permission from ref 158, Copyright 2007 The Optical Society. (B) Multi-step optical waveguide splitter and corresponding profile of light path. Adapted with permission from ref 53, Copyright 2018 The Optical Society. (C) Trapping of yeast cells with a dielectric channel waveguide decorated by an array of gold disks acting as plasmonic traps. Adapted with permission from ref 147. Copyright 2011 AIP Publishing.

Wang's group has carried out a series of work concerning the manipulation of particles based on the optical waveguide.¹⁶³⁻¹⁶⁵ They proposed a configuration for the delivery and trapping of nanoscale polystyrene sphere (40 nm).⁹⁴ This system is consisting of three basic components: a waveguide in the bottom (Si), a layer of SiO₂ right above the waveguide with a channel in the middle, and graded silver nanorod dimers embedded in the SiO₂ layer. All nanorod dimers are fabricated with the same thickness, length, and gap distance. However, the widths are designed differently to make the nanodimers with different resonance wavelengths. As a result, the target nanoparticles can be transferred forward/backward or trapped in a location by changing the incident wavelength. Wong *et al.* reported an optical trapping platform by decorating an array of gold microdisks on the top of the optical waveguide (see Figure 6C).¹⁴⁷ They found that the delivery speed of the targeted polystyrene sphere can reach up to 4.5 μm/s for waveguide coupling, compared to 0.4 μm/s for the prism coupling. Accordingly, the mean trapping time needed is reduced to about one-third of the traditional prism coupling configuration. Similarly, Lin *et al.* numerically and experimentally demonstrated a trapping configuration by combining waveguides and bowtie structures, which can trap the polystyrene sphere as large as 1 μm.⁸⁴ The motions of the particles are induced by the optical force of an evanescent wave around the waveguide. This principle is also adopted in other applications such as particle sorting.^{94, 165, 166}

Another advantage of the waveguide-based method is that it can be easily integrated with other techniques to improve the performance of the trapping or sorting activities.¹⁶⁷⁻¹⁶⁹ Zheng *et al.* developed a hybrid photothermal waveguide to realize the trapping of suspended particles with a tunable position.¹⁰² The system allows the transition of the fluid transport model from thermal-induced buoyancy to thermocapillary convection, which can achieve 3D manipulation of particles. Renaut *et al.* proposed an optical tweezer technique that can realize the reshaping of the optical

traps by tuning the wavelength of the external light source.¹⁷⁰ This is achieved by integrating a set of coupled cavities with the microfluidic cell. Furthermore, different functions, such as trapping, moving, and rotating of particles can be obtained by tuning the pattern of the optical trap.

Beyond the waveguide-based method, another technique named as nano-optical conveyor belt (NOCB) is also investigated in POT to transport target particles (see Figure 7). Usually, the configuration of the NOCB system consists of a metasurface decorated by anisotropic nanostructures and an excitation beam with rotatable polarization states.⁹⁷ Since the metasurface covers a very large area, it is reasonable to assume the target particles already around the plasmonic structures. Therefore, in this situation, the delivery means the controlled motion of particles on the metasurface. Under light illumination, the localized field enhancement of a nanostructure can be excited to trap target particles in the hotspots. The position of the hotspots can be tuned continuously by altering the polarization direction or the wavelength of the incident light for anisotropic nanostructures, resulting in the handoff of target particles between different trapping positions. The most important part to implement this method is the design of the metasurface. Wang and coworkers developed several different plasmonic metasurfaces, including nano-ellipses array and non-concentric nanorings array (see Figure 7A and Figure 7B), to realize two-dimensional transport of nanoparticles by rotating the polarization direction of the incident laser beam.^{97, 171} More complicated configurations have also been developed (see Figure 7C).^{172, 173} Moreover, the transport of particles can also be achieved without steering the incident light by taking advantage of the anisotropic configuration of plasmonic nanostructure induced lateral optical forces (see Figure 7D).¹⁷⁴ Therefore, programmable and arbitrary 2D manipulation of particles are obtained by carefully designing the nanostructures.^{94, 171-173, 175} This configuration has an inherent filtering capability that can be used for delivering, sorting, and trapping operations.¹⁷² Compared to the

waveguide-based method, this metasurface-based method has relatively higher delivery efficiency (conveyor speed), as a result of the enhanced optical force. However, the operation area is relatively small and limited to the light illuminated spot.

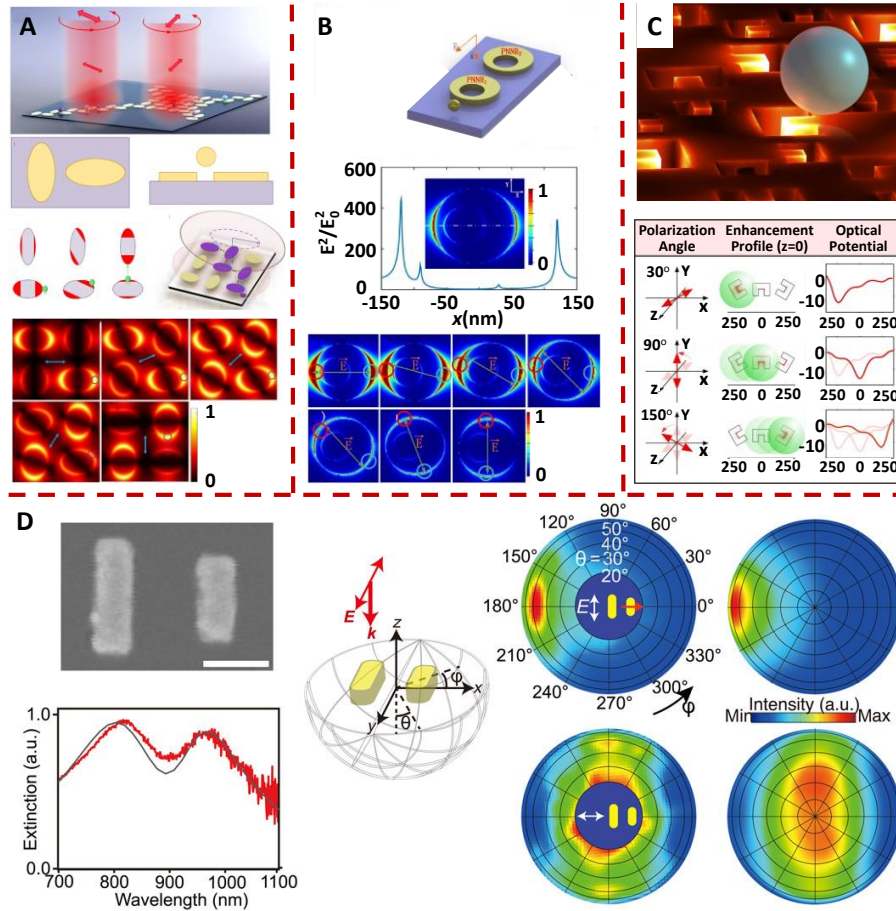


Figure 7. Nano-optical conveyor belt. (A) Two-dimensional arbitrary nano-manipulation on a plasmonic metasurface and the particles motion along the elliptical element and transport between two adjacent ones. Adapted with permission from ref 97. Copyright 2018 The Optical Society. (B) Plasmonic non-concentric nanorings array as a unidirectional nano-optical conveyor belt actuated by polarization rotation. The figures at the bottom illustrate the electric field intensity distribution and trapping spots at different angles of incident polarization. Adapted with permission from ref 171. Copyright 2017 The Optical Society. (C) Transport of polystyrene spheres using nano-optical conveyor belt based on C-shaped plasmonic nanostructures. Adapted

with permission from refs 172 and 173. Copyright 2014 American Chemical Society. (D) Using a pair of nanoparticles with detuned dipolar resonances to generate lateral optical force.

Reprinted from ref 174, whose figures are licensed under Creative Commons Attribution License 4.0 (CC BY).

Motion Induced by Fluid Flow. In this review, the motion induced by fluid flow refers to that the transport of the target particles is dominated by the fluid flow, which can be divided into two categories, the pressure-driven fluid flow, like syringe pump, and other force-field-induced fluid flow, such as temperature gradient and electric field.^{151, 176} The velocity limitation of effective control of particles, using optical tweezer can reach up to a few hundred micrometers per second. This depends on the particle types and components,⁴⁰ and will be higher when the plasmonic structures are applied to enhance the local electromagnetic field. The most apparent advantage of fluid flow induced delivery is its well-controlled delivery speed such as controlling the injected mass flow rate of the sample solutions.

Pressure-driven fluid flow is the most efficient and easy way to deliver target particles to the manipulation area or spot in microfluidics. It is almost applicable for all kinds of situations as the transport of target particles is induced by the fluid drag force, which is label-free, easy-to-control, and does not require any special properties or labeling from the targets. Based on this, Huang *et al.* reported the capturing of yeast cells, using laser irradiated gold microdisks arrays integrated on the bottom of a microfluidic chip.⁹⁰ The experimental setups are shown in Figure 8A. A gold microdisks array is deposited on the glass substrate right under the microflow channel. When the microdisks are irradiated by laser, the optical potential well near the disks will be enhanced, and therefore be able to trap larger objects such as yeast cells (a few microns). However, the liquid flow must be slowed down or even stopped when the particles are transported to the area near the

trapping spot. This severely limits the efficiency and improves the complicity of this device. Therefore, the most promising application of pressure-driven target delivery is not in trapping but high-throughput sorting of micro-/nano-objects. Figure 8B & 8C reveal two typical types of particle sorting microfluidic chips utilizing the pressure-driven target delivery method. The main difference is the laser irradiation directions, *i.e.*, vertical (from the top or bottom) or horizontal irradiation. It is simply comprehended that for horizontal irradiation, the particle sorting is based on the different scales of scattering forces which depend on the particle size and material.¹⁷⁷ As for the vertical irradiation, the different paths of particles can be induced by the asymmetrical distribution of light field, which can be achieved by complex plasmonic structures or varying external conditions. For example, Samadi *et al.* proposed a particle sorting system based on tunable POT by electrostatically changing the chemical potential of two parallel graphene stripes along the microchannel.¹⁴⁵ Then the localized electromagnetic field enhancement can be manipulated accordingly due to the dependence of dielectric properties of graphene on chemical potential. To be specific, the sorting region in the microfluidic chip shown in Figure 8B is illuminated by polarized light. When appropriate bias voltages are applied on one graphene stripe, the corresponding surface plasmons can be excited. Then the generated optical force can be utilized to change the path of the incoming particles, and therefore to realize particle sorting.

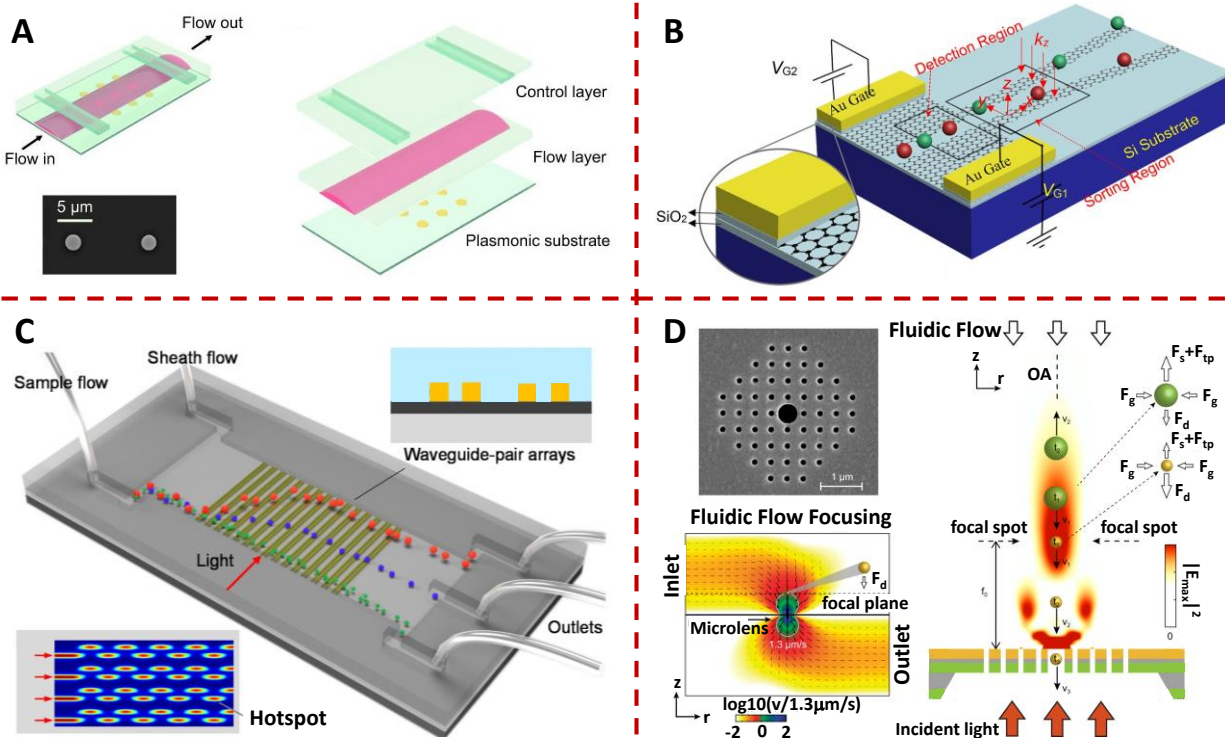


Figure 8. (A) Yeast cell trapping using laser irradiated gold disks array. The chip is made of three layers: the plasmonic substrate, the flow layer, and the control layer. Adapted with permission from ref 90, Copyright 2009 The Optical Society. (B) Tunable plasmonic tweezers based on graphene stripes. Reprinted from ref 145, whose figures are licensed under Creative Commons Attribution License 4.0 (CC BY). (C) Schematic of the silicon waveguide-pair array-based nanophotonic sorting platform. Adapted with permission from ref 177. Copyright 2021 Elsevier. (D) schematic of optofluidic plasmonic microlens consisting of a patch array of small circular nanoholes and an enlarged center aperture for nanofluidic integration. The focal spot region is used to separate two different size particles. Adapted from ref 148, whose figures are licensed under Creative Commons Attribution License 4.0 (CC BY).

Optical chromatography is a powerful tool to realize the label-free separation of microscale bioparticles, such as cells, viruses, and bacteria. The basic principle is to utilize a well-controlled focused laser beam that is precisely aligned along the fluidic channel to create an optical force that

is opposite to the drag force. Since these forces are heavily related to the particle size and refractive index, different kinds of particles can be separated effectively.¹⁷⁸⁻¹⁸⁰ To reduce the complexity of the laser focusing system and laser intensity, Zhu *et al.* proposed a subwavelength thick optofluidic plasmonic microlens to achieve objective free focusing and self-alignment (see Figure 8D).^{148, 181} It was demonstrated numerically that the proposed platform has the potential to be used to separate nanoscale bioparticles from a heterogeneous mixture of different chemical compositions without the need to require complicated experimental equipment, such as laser, objectives and precise alignment stages.^{148, 181} Although the investigated flow speeds are restricted to a few micrometers per second, it has the potential to be further improved.

Besides the pressure-driven fluid flow, there are some other ways to induce well-controlled fluid flow in a microchannel. It has long been recognized that the heating effect and its accompanying phenomena of plasmonic tweezers.¹⁸² However, until very recently, it was considered as a side effect to be suppressed, instead of being exploited.^{118, 183} In the last few years, the idea of using the thermal-induced effects, such as thermal convection, Marangoni convection, thermophoresis, *etc*, has been proposed to improve the delivery efficiency of particle trapping and sorting when utilizing plasmonic optical tweezers.^{57, 60, 102, 150, 184} With the emerging of thermal optofluidics, this delivery method has been widely investigated.⁵⁷ It can be used dependently or combined with other techniques, including opto-thermoelectric tweezers,^{185, 186} opto-thermophoretic tweezers,^{64, 187} and opto-thermo-electrohydrodynamic tweezers.^{96, 150} Particularly, Lin *et al.* developed an opto-thermoelectric tweezer by using extremely low-power laser intensity.¹⁸² The light induced thermoelectric field is applied to dynamically control metal nanoparticles by optically heating the plasmonic substrate, during which the target particles are delivered to the laser spot (see Figure 9A). It was found that this technique is applicable to a wide

range of metal, semiconductor, polymer, and dielectric nanostructure with charged or hydrophobic surfaces. Ndukaife *et al.* introduced a particle trapping system from the combination of photoinduced heating and an a.c. electric field. The transportation of target particles is achieved with the help of eletrothermoplasmonic flow (see Figure 9B).¹⁵⁰ It is found that when only the laser is turned on, the maximum fluid radial velocity in the chamber is 75 nm/s, which is not enough for the fast delivery of particles in practical applications. However, when both laser and a.c. field are simultaneously turned on, the fluid velocity can reach up to 11.8 $\mu\text{m/s}$ (simulation) or 15 $\mu\text{m/s}$ (experiment). Furthermore, in a control experiment, they show that with only the electric field and the laser beam is turned off, no fluid motion is observed. It indicates that a.c. electroosmosis, which arises due to the interaction between an applied electric field and induced free charges in the electrical double layer at a solid–fluid interface, is not the driving mechanism for the observed fluid flow.¹⁵⁰ On this basis, Ndukaife *et al.* further developed a thermoplasmonic metasurface (TPM) platform using nanohole array as optical tweezer (see Figure 9C), which can realize fluid flow of about 20 $\mu\text{m/s}$ at 100 μm away from the nanohole surface.¹⁵¹ We can see that although the above-mentioned methods can achieve the relatively fast delivery of target objects, the effective operating distance is still limited to a few hundred micrometers.

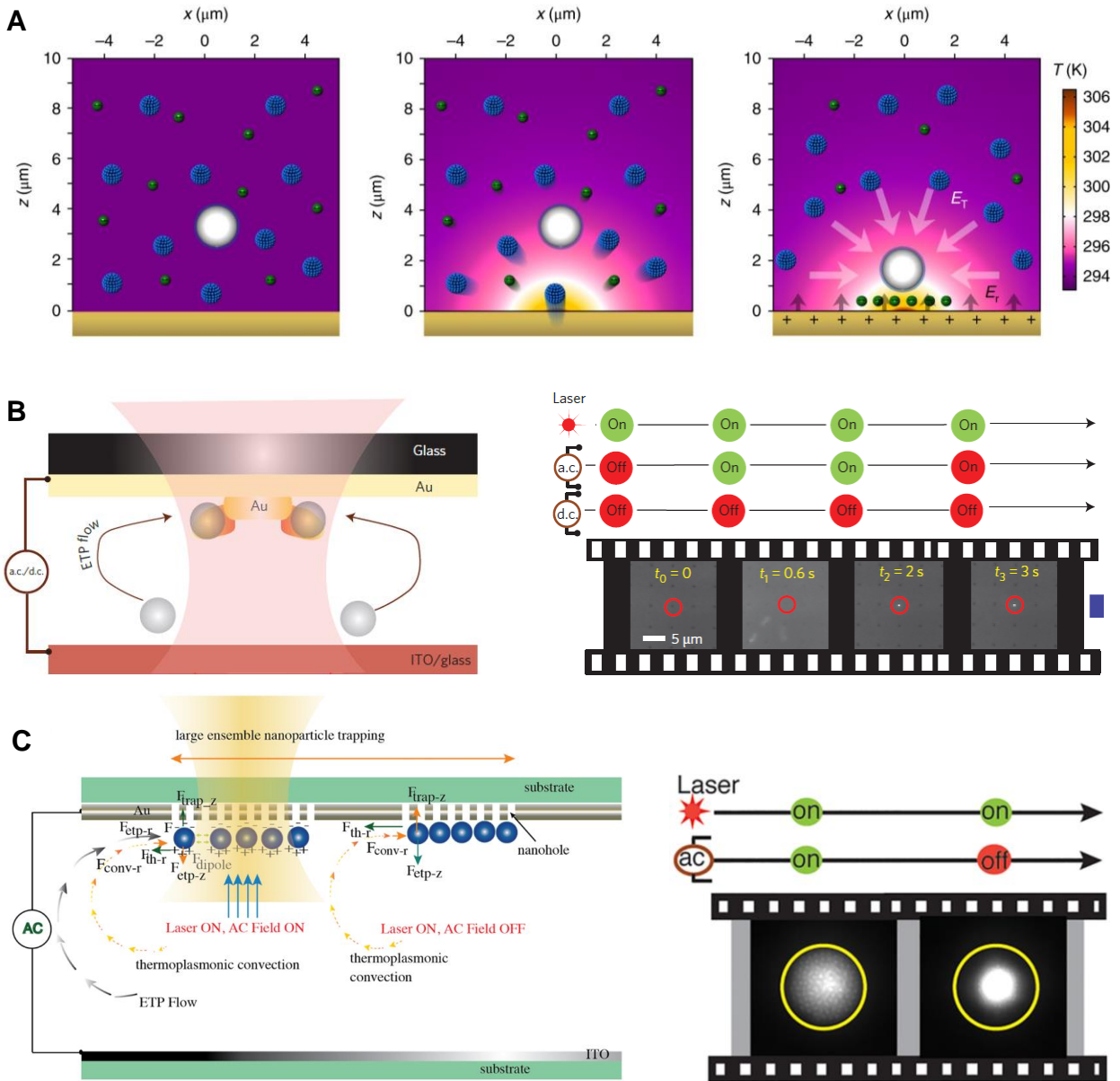


Figure 9. Plasmonic heating assisted delivery. (A) Working principle of opto-thermoelectric nanotweezers. Reprinted with permission from ref 185. Copyright 2018 Springer Nature. (B) Particle trapping and immobilization using nanodisk as plasmonic optical tweezer. When $t = 0$, only the laser is on. When $t = 0.6$ s, the a.c. field is turned on to induce electrothermoplasmonic flow for rapid delivery of particles to the plasmonic hotspot. When $t = 2$ s, a particle is delivered to the hotspot. When the a.c. field is turned off at $t = 3$ s, the particle is captured by the plasmonic tweezer. Adapted with permission from ref 150. Copyright 2015 Nature Publishing Group. (C)

Thermoplasmonic metasurface (TPM) platform using nanohole array as optical tweezer. Trapping forces present in the TPM platform when the laser illumination is ON and AC electric field is either ON or OFF. The electrothermoplasmonic flow arises from the combined action of the induced thermal gradient and applied AC electric field. Reprinted with permission from ref 151. Copyright 2018 American Chemical Society.

Motion of Target Particles Induced by Other External Forces. Besides the waveguide-based method, there are also other ways to directly propel the target particles without the help of fluid flow, *i.e.*, the mobile nanotweezers. In this technique, the target particles are trapped around the mobile plasmonic micro-/nano-structure rather than a pre-defined spot as a result of the optical tweezer effect.⁴⁴ Afterward, the mobile nanotweezers with target particles can be manipulated and transferred to the desired area, through external forces, such as magnetic actuation¹⁸⁸ and acoustic propulsion.¹⁸⁹ As mentioned above, the microrobots can act as a trapping point and deliver the vehicle at the same time, which makes the delivery of the targets become selective and label-free (see Figure 10). A typical type of mobile nanotweezers comprises two parts, including the trapping points normally consisting of plasmonic materials, and the “motor” providing power for the transportation of the cargo (see Figure 10A & 10B). In this situation, the delivering speed will be limited by the strength of external propulsive force instead of the optical trapping force, which will be a promising technique for the improvement of delivery efficiency. Moreover, the power of mobile nanotweezers also can be mechanical forces.³⁵ By integrating the POT at the end of optical fiber, the target particles can be delivered by simply moving the fiber (see Figure 10C). It should be noted that, in this situation, there are two delivery methods. One is that the target particles first need to be diffused to the end of the optical fiber. The other is the mechanical delivery after the particle is trapped. More importantly, the mobile POT successfully transfers the nearly 2D trapping

and delivering into a 3D problem. It means that the manipulation of targets occurs in the bulk fluid rather than the thin layer of fluid near the nanostructure surface. Furthermore, beyond the remote control through light, magnetism, or acoustics, the mobile nanotweezers can also be controlled by contact methods such as mechanical force. Berthelot *et al.* realized a 3D optical manipulation of nano-objects by engineering a plasmonic bowtie structure at the extremity of optical fiber.³⁵ After trapping the target particles at the optical trap induced by the plasmonic structure, the optical fiber can be moved utilizing high-precision translation stages. The operation precision can be well controlled while reducing the light intensity by several orders of magnitude compared to traditional optical tweezers. However, the moving speed is relatively low in comparison with the remote-control methods.

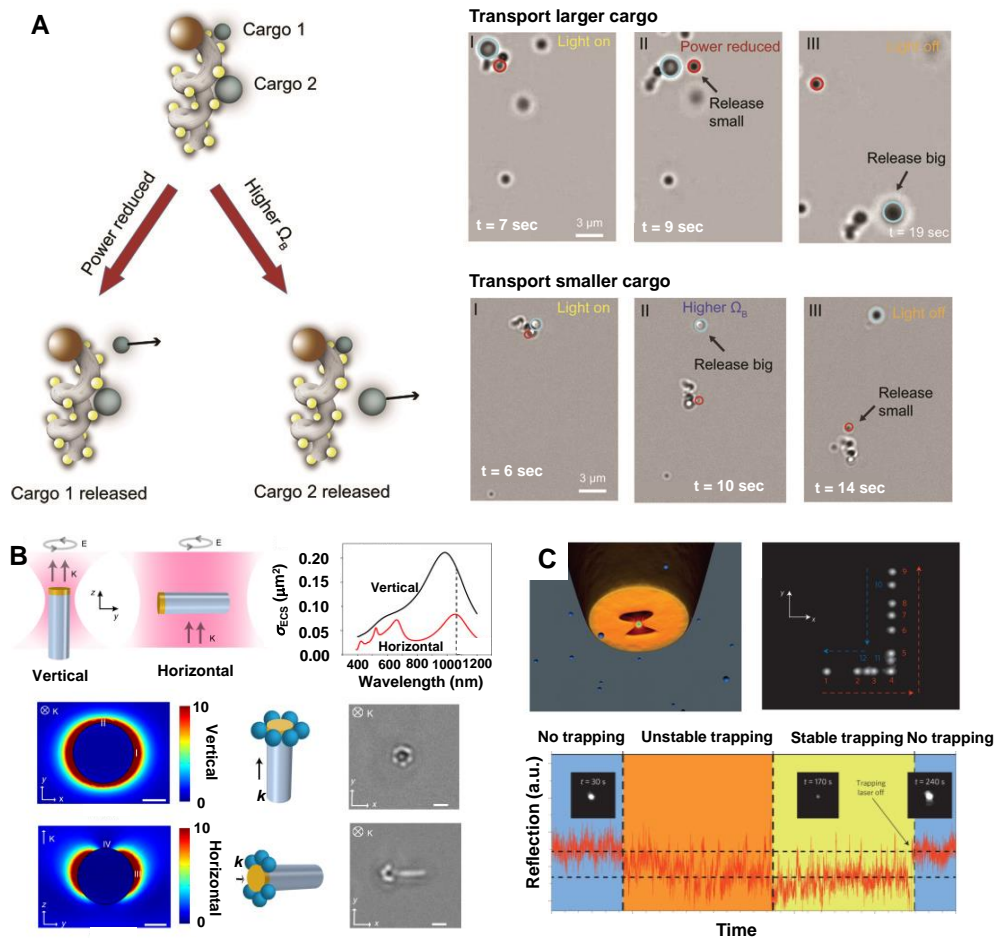


Figure 10. Mobile nano-tweezer. (A) Magnetized helical nanostructure with plasmonic head. Under light illumination, the plasmonic head can trap small particles. At the same time, the helical structure can be propelled by a rotating magnetic field to be delivered to target location. Adapted with permission from ref 99. Copyright 2018 American Association for the Advancement of Science. (B) Dynamic nanomanipulation with light-controlled active colloidal tweezers. The dielectric microrods with plasmonic heads that can be manipulated by conventional optical tweezers act like vehicles to deliver the target nanoscale particles. Adapted from ref 31, whose figures are licensed under Creative Commons Attribution License 4.0 (CC BY). (C) Three-dimensional manipulation of a single 50 nm polystyrene bead with scanning near-field optical nanotweezers. The trapping laser is directly coupled into the fiber to excite the transverse mode of the bowtie nano-aperture. After being trapped, the target particles can be delivered directly by mechanical forces acting on the optical fiber. Adapted with permission from ref 35. Copyright 2014 Nature Publishing Group.

APPLICATIONS

Due to its simple configuration, the POT is very easy to be integrated with other techniques. The most promising opportunity for POT lays in the biological applications, *in vivo* and *in vitro*, such as single cell or molecule imaging and analysis, bioparticles purifying, targeted drug delivery and release, *etc.*¹⁹⁰⁻¹⁹³ In this section, some state-of-the-art applications and promising potential applications are introduced.

Single Bioparticle Analysis. POT can be easily integrated with lab-on-chip technologies and apply for single-molecule analysis. Meanwhile, besides the advantage of enhancing the surface plasmon, and therefore to break the limitation of conventional optical tweezers, the plasmonic structures can be conveniently combined with other plasmonic-based applications, such as

acceleration of photo-/thermal-chemical reactions and chemical/biological sensing.¹⁹⁴⁻¹⁹⁷ For example, Raman spectroscopy is an approach that is frequently used to analyze the fingerprint information of molecular structure and chemical composition. However, these scattering signals of a single molecule or even molecule ensembles are too weak and unstable for detection.¹⁹⁸ Surface-enhanced Raman scattering (SERS) spectroscopy, which represents a technique that using plasmonic nanostructures or rough metal surfaces to enhance the Raman scattering (as high as 10^{10} to 10^{15} times^{198, 199}). Consequently, it makes the signal detectable for a single molecule. Therefore, plasmonic nanostructures utilized in the POT can be beneficial for the SERS at the same time.²⁰⁰ Most importantly, when integrating the POT with SERS measurement systems, the optical trapping function of the POT technique can tackle the Brownian motion of molecules and finally significantly improve the reproducibility of the SERS.^{121, 201} The accompanying accumulation of molecules or nanoparticles attached with molecules will also contribute to the Raman scattering enhancement (see Figure 11). Besides SERS spectroscopy, POT can also be integrated with other probing techniques for small bioparticles, such as viruses or bacteria which are beyond the diffraction limits.^{202, 203} For example, the diameter of coronavirus 2 (SARS-CoV-2) is in the range of 60 to 140 nm.²⁰⁴ The application of the POT technique not only traps the targets in a predefined location but also enhances the detection signals.

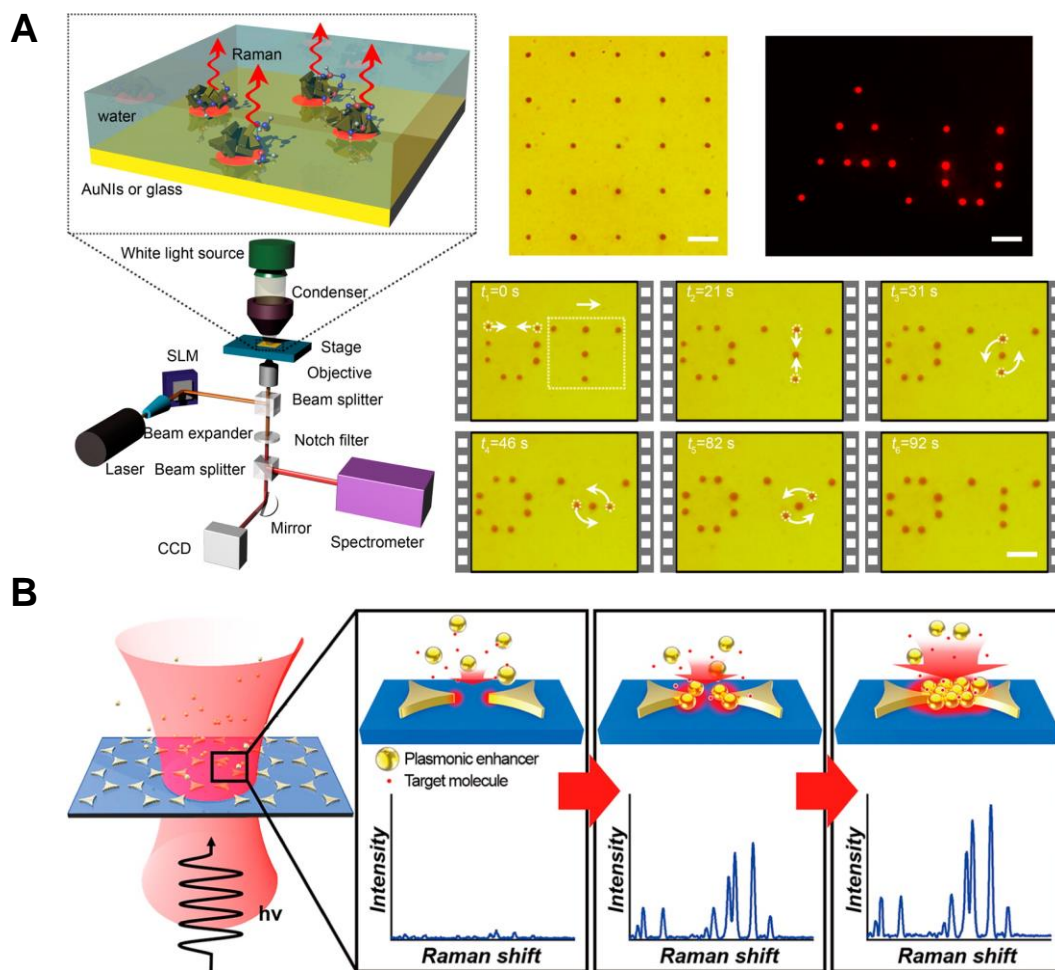


Figure 11. Signal enhancement of POT integrated with SERS spectroscopy. (A) Light-directed reversible assembly of plasmonic nanoparticles using plasmon enhanced thermophoresis. Reprinted with permission from ref 205. Copyright 2016 American Chemical Society. (B) Autoenhanced Raman spectroscopy *via* plasmonic trapping for molecular sensing. Reprinted with permission from ref 121. Copyright 2016 American Chemical Society.

High-Throughput Bioparticles Purification. High-throughput bioparticles (cells or viruses) sorting is a critical issue for many applications including biology, medicine, and clinical diagnostics/therapy.²⁰⁶⁻²⁰⁹ Bioparticles sorting refers to one kind of technologies that enables the sorting of target cells or viruses from complex and heterogeneous mixtures such as purifying cells into pure populations.⁶⁶ One commercialized and relatively mature cell sorting technique is

fluorescence-activated cell sorting, which was proposed by Herzenberg *et al.*,²¹⁰ and now it has been used as a benchmark for cell sorting techniques.⁶⁶ However, this technique suffers from drawbacks such as the requirement of a very large sample volume and high operation cost. Meanwhile, to avoid sample contamination, elaborate cleaning and maintenance procedures are mandatory and complex.²¹¹ More importantly, this technique is only applicable to cells that can be specially labeled, which seriously restricts its application.²⁰⁶ To overcome those problems, different strategies have been proposed, where the microfluidics-based techniques are the most popular and promising,²¹² *i.e.*, POT-based microfluidic chips.^{16, 116, 148} But still, compared to other relatively well-developed lab-on-chip cell sorting techniques which are based on other active or passive mechanisms (such as electrokinetic or mechanical effects), there remains a lot of work to be done.⁶⁶

Label-Free Single Bioparticle Imaging. Till now, fluorescent imaging is the most widely used technique for the imaging of subwavelength objects. This approach has achieved nearly single-molecular-level resolution, such as stimulated emission depletion and photo-activated localization microscopy.²¹³⁻²¹⁶ However, similar to the fluorescence-activated cell sorting technique, it is seriously limited by the fluorescent labeling process. Furthermore, the photobleaching effect will reduce the signal-to-noise ratio since the number of available photons is limited.³⁷ Therefore, the development of a label-free subwavelength bioparticle imaging technique is crucially important. Second-harmonic imaging is a label-free technique that is based on a nonlinear optical effect named second harmonic generation (SHG). SHG does not need the excitation of molecules to provide fluorescence, which means it does not suffer from the side effect of phototoxicity and photobleaching.^{217, 218} Hence, it becomes a promising alternative imaging technique. Recently, the idea of further enhancement of SHG utilizing the tightly confined electromagnetic field induced

by plasmonic nanostructures has attracted more and more attention.²¹⁹⁻²²¹ By integration with POT, the performance of second harmonic imaging can be further improved with the target strictly confined in the hotspot of the plasmonic nanostructures.

Single-Atom Manipulation. Atomic manipulation is a process of manipulating precisely controlled single atom on a substrate to build up artificial objects or realized certain objects. It was achieved by Eigler and Schweizer using a scanning tunneling microscope in 1990.²²² Since then, it has been investigated and developed by many researchers.²²³⁻²²⁵ Recently, conceptual and experimental work has shown that the manipulation of a single atom through plasmonic optical tweezers is possible.^{226, 227} It has been proven that plasmonic nanostructures can further permit complex trap geometries, such as lattice heterostructures and Fibonacci lattices.²²⁷ Extension of plasmonic tweezers application into this field is promising as an alternative method of higher levels of integration.²⁹

Light-Driven Micro-/Nano-Robots. Another very interesting and exciting application is the light-driven micro-/nano-robots (MNRs) which refers to a kind of micro-/nano-object that can be propelled by light.^{146, 228} The motion of MNRs is induced by converting light into mechanical work, including light-induced phoretic propulsion, bubble recoil, thermophoresis, interfacial tension gradient, *etc.*¹⁴⁶ Generally, it requires asymmetric Janus structures or other asymmetric structures.^{229, 230} Also, the rapid development of light-driven micro-/nano-robots is inspiring for the further development of the mobile delivery method for particle sorting and trapping devices. As-mentioned, the MNRs can act as carriers of the target objects to improve delivery efficiency.⁹⁹ Meanwhile, the targets do not need to be labeled since the MNRs can be integrated with POT, to trap the target onto the MNRs. Moreover, this technique can be further extended to *in vivo* applications like targeted/smart drug delivery and release.

CHALLENGES AND PERSPECTIVES

In contrast to traditional optical tweezers, POT techniques have the ability to confine an enhanced electromagnetic field at the nanoscale level. Therefore, it can break the diffraction limits and improve the manipulation precision of traditional optical tweezers to nanoscale level with a stronger optical force and potential well.²⁹ Moreover, this technique has lots of applications in the fields of single-cell/molecule/atom analyzing and manipulation. Meanwhile, it has also brought some topics that need to be addressed, such as the mechanism of localized electromagnetic field enhancement and precise nanoscale object manipulation. More importantly, unlike traditional optical tweezers, the operation spots of POT are often located in a predefined area, which makes the target delivery to become a crucial issue that needs to be investigated. In this review, the basic principles of POT for manipulating micro-/nano-objects are introduced, and the state-of-the-art advancement of delivery methods and applications are summarized. Due to apparent advantages, such as high spatial resolution, ease to integrate with other techniques, *etc.*, POTs have been widely investigated in the last few decades, and massive progress and achievements have been made in related fields. However, there are still some limitations and challenges that need to be clarified.

In the applications of plasmonic optical tweezers, the heat generation and corresponding effects induced by the light-matter interactions, such as fluid convection, thermophoresis, and Margoni effect, should be treated carefully.^{58, 137, 231} Sometimes, it may be a barrier for the accurate manipulation of particles.²³² However, it could also provide a solution for the efficient delivery of nano-objects by combining with other techniques, including opto-thermoelectric tweezers, opto-thermophoretic tweezers, opto-thermo-electrohydrodynamic tweezers, *etc.* Since the optical forces acting on a sphere are proportional to the third power of the particle radius,²⁹ it would be beneficial to combine with other forces when manipulating particles with a radius of a few tens of nanometers

or sub-10 nm.⁹⁶ Meanwhile, most of the applications of POT are focused on the trapping effect. As a very important application, investigations related to particle sorting or purification using POT seem to be ignored, which, on the other hand, has been achieved with the help of traditional optical tweezers technique.⁶⁶ By adopting the POT technique, the precision and efficiency could be further improved, especially for small bioparticles like viruses or even smaller molecules. More importantly, although the configurations of POT are relatively simple and easy to achieve, more work should be done to further simplify this technique. One of the potential directions is electrically activated lab-on-a-chip plasmonic tweezers, which do not require an external light source. This kind of device consists of an array of plasmonic nanostructures and a base layer of quantum cascaded heterostructures or other structures, to act as built-in optical sources to excite the localized surface plasmon.⁵⁴ The main advantage of this method is that it does not require expensive and complex external light sources, which is very important for the application of on-chip plasmonic optical tweezers.

Although manipulation of plasmonic particles using traditional optical tweezers has been widely investigated,¹¹⁰⁻¹¹² trapping and sorting of plasmonic particles using POT are relatively not so well investigated compared to that of dielectric particles. The reason behind this is the similarity of dielectric particles with bioparticles, and therefore have a wider application. Besides, due to the interaction between the target plasmonic particles and the plasmonic structure of optical tweezers, it is more complicated to stably manipulate plasmonic particles using this technique. Therefore, further development of using other forces to assist the POT-based manipulation of plasmonic particles also needs further investigation. For example, thermal optofluidic is especially effective for the manipulation of plasmonic nanoparticles due to the thermal effects and thermal-induced forces.⁵⁷ Meanwhile, it should be noted that the plasmon enhancement is nearly confined in a

subwavelength volume, near the micro-/nano-structures, while most of the trapping and sorting of particles is a 3D problem. Although it can be partly solved by the mobile nanotweezers techniques,⁹⁹ future work is still recommended for further improvements, such as extending the application of this technique from *in vitro* to *in vivo* or developing more efficient and simpler delivery methods.

ACKNOWLEDGMENTS

The supports of this work by the National Natural Science Foundation of China (No. 51806047), the China Postdoctoral Science Foundation (No. 2019T120264), the Natural Science Foundation of Heilongjiang (LH2019E047), European Union's Horizon 2020 research and innovation programme under the Marie Skłodowska-Curie grant agreement No. 839641 and ThermaSMART project under grant No. H2020-MSCA-RISE-778104 are gratefully acknowledged.

VOCABULARY

mobile nanotweezers, nanotweezers located in a freely moving vehicle in solutions instead of locating in a fixed position; **near-field interaction**, the interaction of strongly confined electric field around each nanostructure between closely packed plasmonic nanostructures; **Maxwell stress tensor**, representing the interaction between electromagnetic forces and mechanical momentum; **surface-enhanced Raman scattering**, a technique for using plasmonic nanostructures or rough metal surfaces to enhance the Raman scattering; **nano-optical conveyor belt**, a metasurface decorated by anisotropic nanostructures for transporting the particles; **hotspot**, a location in an electromagnetic field with a strongly enhanced electromagnetic intensity.

REFERENCES

- (1) Bergman, J.; Osunbayo, O.; Vershinin, M. Constructing 3D Microtubule Networks Using Holographic Optical Trapping. *Sci. Rep-UK* **2015**, *5*, 1-9.
- (2) Maragò, O. M.; Jones, P. H.; Gucciardi, P. G.; Volpe, G.; Ferrari, A. C. Optical Trapping and Manipulation of Nanostructures. *Nat. Nanotechnol.* **2013**, *8*, 807-819.
- (3) Urban, A. S.; Carretero-Palacios, S.; Lutich, A. A.; Lohmuller, T.; Feldmann, J.; Jackel, F. Optical Trapping and Manipulation of Plasmonic Nanoparticles: Fundamentals, Applications, and Perspectives. *Nanoscale* **2014**, *6*, 4458-4474.
- (4) Isozaki, A.; Mikami, H.; Hiramatsu, K.; Sakuma, S.; Kasai, Y.; Iino, T.; Yamano, T.; Yasumoto, A.; Oguchi, Y.; Suzuki, N. A Practical Guide to Intelligent Image-Activated Cell Sorting. *Nat. Protoc.* **2019**, *14*, 2370-2415.
- (5) Lyu, Y.; Yuan, X.; Glidle, A.; Fu, Y.; Furusho, H.; Yang, T.; Yin, H. Automated Raman Based Cell Sorting with 3D Microfluidics. *Lab Chip* **2020**, *20*, 4235-4245.
- (6) Mishra, A.; Dubash, T. D.; Edd, J. F.; Jewett, M. K.; Garre, S. G.; Karabacak, N. M.; Rabe, D. C.; Mutlu, B. R.; Walsh, J. R.; Kapur, R. Ultrahigh-Throughput Magnetic Sorting of Large Blood Volumes for Epitope-Agnostic Isolation of Circulating Tumor Cells. *Proc. Natl. Acad. Sci.* **2020**, *117*, 16839-16847.
- (7) Dusny, C.; Grünberger, A. Microfluidic Single-Cell Analysis in Biotechnology: From Monitoring towards Understanding. *Curr. Opin. Biotechnol.* **2020**, *63*, 26-33.
- (8) Jeffries, G. D.; Edgar, J. S.; Zhao, Y.; Shelby, J. P.; Fong, C.; Chiu, D. T. Using Polarization-Shaped Optical Vortex Traps for Single-Cell Nanosurgery. *Nano Lett.* **2007**, *7*, 415-420.
- (9) Gao, D.; Jin, F.; Zhou, M.; Jiang, Y. Recent Advances in Single Cell Manipulation and Biochemical Analysis on Microfluidics. *Analyst* **2019**, *144*, 766-781.

- (10) Gautam, R.; Xiang, Y.; Lamstein, J.; Liang, Y.; Bezryadina, A.; Liang, G.; Hansson, T.; Wetzal, B.; Preece, D.; White, A.; Silverman, M.; Kazarian, S.; Xu, J.; Morandotti, R.; Chen, Z. Optical Force-Induced Nonlinearity and Self-Guiding of Light in Human Red Blood Cell Suspensions. *Light-Sci. Appl.* **2019**, *8*, 31.
- (11) Soltani, M.; Lin, J.; Forties, R. A.; Inman, J. T.; Saraf, S. N.; Fulbright, R. M.; Lipson, M.; Wang, M. D. Nanophotonic Trapping for Precise Manipulation of Biomolecular Arrays. *Nat. Nanotechnol.* **2014**, *9*, 448-452.
- (12) Albrecht, T. Single-Molecule Analysis with Solid-State Nanopores. *Annu. Rev. Anal. Chem.* **2019**, *12*, 371-387.
- (13) Choi, S. S.; Park, M. J.; Lee, Y. M.; Bae, B. S.; Kim, H. T.; Choi, S. B. Fabrication of the Au Nano-Aperture Array Platform for Single Molecule Analysis. *ECS J. Solid State Sc.* **2020**, *9*, 115015.
- (14) Chiriaco, M. S.; Bianco, M.; Nigro, A.; Primiceri, E.; Ferrara, F.; Romano, A.; Quattrini, A.; Furlan, R.; Arima, V.; Maruccio, G. Lab-on-Chip for Exosomes and Microvesicles Detection and Characterization. *Sensors (Basel)* **2018**, *18*, 3175.
- (15) Al Balushi, A. A.; Kotnala, A.; Wheaton, S.; Gelfand, R. M.; Rajashekara, Y.; Gordon, R. Label-Free Free-Solution Nanoaperture Optical Tweezers for Single Molecule Protein Studies. *Analyst* **2015**, *140*, 4760-4778.
- (16) Ndukaife, J. C.; Mishra, A.; Guler, U.; Nnanna, A. G. A.; Wereley, S. T.; Boltasseva, A. Photothermal Heating Enabled by Plasmonic Nanostructures for Electrokinetic Manipulation and Sorting of Particles. *ACS Nano* **2014**, *8*, 9035-9043.

- (17) Yazbeck, R.; Alibakhshi, M. A.; Von Schoppe, J.; Ekinici, K. L.; Duan, C. Characterization and Manipulation of Single Nanoparticles Using a Nanopore-Based Electrokinetic Tweezer. *Nanoscale* **2019**, *11*, 22924-22931.
- (18) Cao, Q.; Fan, Q.; Chen, Q.; Liu, C.; Han, X.; Li, L. Recent Advances in Manipulation of Micro- and Nano-Objects with Magnetic Fields at Small Scales. *Mater. Horiz.* **2020**, *7*, 638-666.
- (19) Snezhko, A.; Aranson, I. S. Magnetic Manipulation of Self-Assembled Colloidal Asters. *Nat Mater* **2011**, *10*, 698-703.
- (20) Zhao, W.; Cheng, R.; Miller, J. R.; Mao, L. Label-Free Microfluidic Manipulation of Particles and Cells in Magnetic Liquids. *Adv. Funct. Mater.* **2016**, *26*, 3916-3932.
- (21) Zhu, T.; Cheng, R.; Lee, S. A.; Rajaraman, E.; Eiteman, M. A.; Querec, T. D.; Unger, E. R.; Mao, L. Continuous-Flow Ferrohydrodynamic Sorting of Particles and Cells in Microfluidic Devices. *Microfluid. Nanofluid.* **2012**, *13*, 645-654.
- (22) Volpe, A.; Gaudiuso, C.; Ancona, A. Sorting of Particles Using Inertial Focusing and Laminar Vortex Technology: A Review. *Micromachines* **2019**, *10*, 594.
- (23) Shilkin, D. A.; Lyubin, E. V.; Shcherbakov, M. R.; Lapine, M.; Fedyanin, A. A. Directional Optical Sorting of Silicon Nanoparticles. *ACS Photonics* **2017**, *4*, 2312-2319.
- (24) Wang, X.; Chen, S.; Kong, M.; Wang, Z.; Costa, K. D.; Li, R. A.; Sun, D. Enhanced Cell Sorting and Manipulation with Combined Optical Tweezer and Microfluidic Chip Technologies. *Lab Chip* **2011**, *11*, 3656-3662.
- (25) MacDonald, M. P.; Spalding, G. C.; Dholakia, K. Microfluidic Sorting in an Optical Lattice. *Nature* **2003**, *426*, 421-424.
- (26) Ashkin, A.; Dziedzic, J. M.; Yamane, T. Optical Trapping and Manipulation of Single Cells Using Infrared Laser Beams. *Nature* **1987**, *330*, 769-771.

- (27) Ashkin, A. Acceleration and Trapping of Particles by Radiation Pressure. *Phys. Rev. Lett.* **1970**, *24*, 156.
- (28) Huang, J. S.; Yang, Y. T. Origin and Future of Plasmonic Optical Tweezers. *Nanomaterials (Basel)* **2015**, *5*, 1048-1065.
- (29) Crozier, K. B. *Quo Vadis*, Plasmonic Optical Tweezers? *Light-Sci. Appl.* **2019**, *8*, 35.
- (30) Zhang, J.; Lu, F.; Zhang, W.; Yu, W.; Zhu, W.; Premaratne, M.; Mei, T.; Xiao, F.; Zhao, J. Optical Trapping of Single Nano-Size Particles Using a Plasmonic Nanocavity. *J. Phys-Condens. Mat.* **2020**, *32*, 475301.
- (31) Ghosh, S.; Ghosh, A. All Optical Dynamic Nanomanipulation with Active Colloidal Tweezers. *Nat. Commun.* **2019**, *10*, 4191.
- (32) Zhang, W.; Huang, L.; Santschi, C.; Martin, O. J. Trapping and Sensing 10nm Metal Nanoparticles Using Plasmonic Dipole Antennas. *Nano Lett.* **2010**, *10*, 1006-1011.
- (33) Tan, H.; Hu, H.; Huang, L.; Qian, K. Plasmonic Tweezers for Optical Manipulation and Biomedical Applications. *Analyst* **2020**, *145*, 5699-5712.
- (34) Xu, H.; Jones, S.; Choi, B. C.; Gordon, R. Characterization of Individual Magnetic Nanoparticles in Solution by Double Nanohole Optical Tweezers. *Nano Lett.* **2016**, *16*, 2639-2643.
- (35) Berthelot, J.; Aćimović, S.; Juan, M.; Kreuzer, M.; Renger, J.; Quidant, R. Three-Dimensional Manipulation with Scanning Near-Field Optical Nanotweezers. *Nat. Nanotechnol.* **2014**, *9*, 295-299.
- (36) Jin, R. C.; Li, J. Q.; Li, L.; Dong, Z. G.; Liu, Y. Dual-Mode Subwavelength Trapping by Plasmonic Tweezers Based on V-Type Nanoantennas. *Opt. Lett.* **2019**, *44*, 319-322.

- (37) Kotsifaki, D. G.; Chormaic, S. N. Plasmonic Optical Tweezers Based on Nanostructures: Fundamentals, Advances and Prospects. *Nanophotonics* **2019**, *8*, 1227-1245.
- (38) Sun, X.; Li, H. A Review: Nanofabrication of Surface-Enhanced Raman Spectroscopy (SERS) Substrates. *Curr. Nanosci.* **2016**, *12*, 175-183.
- (39) Henzie, J.; Lee, J.; Lee, M. H.; Hasan, W.; Odom, T. W. Nanofabrication of Plasmonic Structures. *Annu. Rev. Phys. Chem.* **2009**, *60*, 147-165.
- (40) Melzer, J. E.; McLeod, E. Fundamental Limits of Optical Tweezer Nanoparticle Manipulation Speeds. *ACS Nano* **2018**, *12*, 2440-2447.
- (41) Wang, L.; Wu, Y.; Wu, X.; Cen, K. Measurement of Dynamics of Laser-Induced Cavitation around Nanoparticle with High-Speed Digital Holographic Microscopy. *Exp. Therm. Fluid Sci.* **2021**, *121*, 110266.
- (42) Boulais, E. T.; Lachaine, R. M.; Meunier, M. Plasma Mediated Off-Resonance Plasmonic Enhanced Ultrafast Laser-Induced Nanocavitation. *Nano Lett.* **2012**, *12*, 4763-4769.
- (43) Karim, F.; Smith, T. B.; Zhao, C. Review of Optical Detection of Single Molecules beyond the Diffraction and Diffusion Limit Using Plasmonic Nanostructures. *J. Nanophotonics* **2017**, *12*, 012504.
- (44) Ghosh, S.; Ghosh, A. Next-Generation Optical Nanotweezers for Dynamic Manipulation: From Surface to Bulk. *Langmuir* **2020**, *36*, 5691-5708.
- (45) Yang, H.; Gijs, M. A. M. Micro-Optics for Microfluidic Analytical Applications. *Chem Soc Rev* **2018**, *47*, 1391-1458.
- (46) Rohrbach, A.; Stelzer, E. H. Optical Trapping of Dielectric Particles in Arbitrary Fields. *J. Opt. Soc. Am. A* **2001**, *18*, 839-853.

- (47) Harada, Y.; Asakura, T. Radiation Forces on a Dielectric Sphere in the Rayleigh Scattering Regime. *Opt. Commun.* **1996**, *124*, 529-541.
- (48) Yang, X.; Liu, Y.; Oulton, R. F.; Yin, X.; Zhang, X. Optical Forces in Hybrid Plasmonic Waveguides. *Nano Lett.* **2011**, *11*, 321-328.
- (49) Wan, T.; Tang, B. Efficient Prediction and Analysis of Optical Trapping at Nanoscale via Finite Element Tearing and Interconnecting Method. *Nanoscale Res. Lett.* **2019**, *14*, 294.
- (50) Ghorbanzadeh, M.; Darbari, S.; Moravvej-Farshi, M. K. Graphene-Based Plasmonic Force Switch. *Appl. Phys. Lett.* **2016**, *108*, 111105.
- (51) Novotny, L.; Bian, R. X.; Xie, X. S. Theory of Nanometric Optical Tweezers. *Phys. Rev. Lett.* **1997**, *79*, 645.
- (52) Xu, W.; Wang, Y.; Jiao, W.; Wang, F.; Xu, X.; Jiang, M.; Ho, H. P.; Wang, G. Tunable Optofluidic Sorting and Manipulation on Micro-Ring Resonators from a Statistics Perspective. *Opt. Lett.* **2019**, *44*, 3226-3229.
- (53) Xu, X.; Wang, G.; Jiao, W.; Ji, W.; Jiang, M.; Zhang, X. Multi-Level Sorting of Nanoparticles on Multi-Step Optical Waveguide Splitter. *Opt. Express* **2018**, *26*, 29262-29271.
- (54) Khorami, A. A.; Moravvej Farshi, M. K.; Darbari, S. Ultralow-Power Electrically Activated Lab-on-a-Chip Plasmonic Tweezers. *Phys. Rev. Appl.* **2020**, *13*, 024072.
- (55) Ashkin, A.; Dziedzic, J. M.; Bjorkholm, J. E.; Chu, S. Observation of a Single-Beam Gradient Force Optical Trap for Dielectric Particles. *Opt. Lett.* **1986**, *11*, 288-290.
- (56) Ren, Y.; Qi, H.; Chen, Q.; Li, Y.; Ruan, L. Optofluidic Control Using Light Illuminated Plasmonic Nanostructure as Microvalve. *Int. J. Heat Mass Tran.* **2019**, *133*, 1019-1025.
- (57) Chen, J.; Loo, J. F. C.; Wang, D.; Zhang, Y.; Kong, S. K.; Ho, H. P. Thermal Optofluidics: Principles and Applications. *Adv. Opt. Mater.* **2019**, 1900829.

- (58) Donner, J. S.; Baffou, G.; McCloskey, D.; Quidant, R. Plasmon-Assisted Optofluidics. *ACS Nano* **2011**, *5*, 5457-5462.
- (59) Namura, K.; Nakajima, K.; Suzuki, M. Investigation of Transition from Thermal- to Solutal-Marangoni Flow in Dilute Alcohol/Water Mixtures Using Nano-Plasmonic Heaters. *Nanotechnology* **2018**, *29*, 065201.
- (60) Winterer, F.; Maier, C. M.; Pernpeintner, C.; Lohmuller, T. Optofluidic Transport and Manipulation of Plasmonic Nanoparticles by Thermocapillary Convection. *Soft Matter* **2018**, *14*, 628-634.
- (61) Michaelides, E. E. Brownian Movement and Thermophoresis of Nanoparticles in Liquids. *Int. J. Heat Mass Tran.* **2015**, *81*, 179-187.
- (62) Michaelides, E. E. S. *Heat and Mass Transfer in Particulate Suspensions*, Springer: New York, USA, 2013; pp 121-158.
- (63) Yang, M.; Ripoll, M. Simulations of Thermophoretic Nanoswimmers. *Phys. Rev. E* **2011**, *84*, 061401.
- (64) Setoura, K.; Tsuji, T.; Ito, S.; Kawano, S.; Miyasaka, H. Opto-Thermophoretic Separation and Trapping of Plasmonic Nanoparticles. *Nanoscale* **2019**, *11*, 21093-21102.
- (65) Jiang, Q.; Rogez, B.; Claude, J.-B.; Baffou, G.; Wenger, J. Quantifying the Role of the Surfactant and the Thermophoretic Force in Plasmonic Nano-Optical Trapping. *Nano Lett.* **2020**, *20*, 8811-8817.
- (66) Shields, C. W. t.; Reyes, C. D.; Lopez, G. P. Microfluidic Cell Sorting: A Review of the Advances in the Separation of Cells from Debulking to Rare Cell Isolation. *Lab Chip* **2015**, *15*, 1230-1249.

- (67) Juan, M. L.; Righini, M.; Quidant, R. Plasmon Nano-Optical Tweezers. *Nat. Photonics* **2011**, *5*, 349-356.
- (68) Lalisse, A.; Tessier, G.; Plain, J.; Baffou, G. Quantifying the Efficiency of Plasmonic Materials for Near-Field Enhancement and Photothermal Conversion. *J. Phys. Chem. C* **2015**, *119*, 25518-25528.
- (69) Ploschner, M. The Role of the Plasmon Resonance for Enhanced Optical Forces. Doctor of Philosophy, University of St Andrews, St Andrews, Scotland, 2012.
- (70) Bondeson, A.; Rylander, T.; Ingelström, P. *Computational Electromagnetics*, 2nd ed.; Springer: New York, USA, 2012; pp 1-231.
- (71) Stratton, J. A. *Electromagnetic Theory*, John Wiley & Sons: New Jersey, USA, 2007; pp 1-6.
- (72) Yee, K. Numerical Solution of Initial Boundary Value Problems Involving Maxwell's Equations in Isotropic Media. *IEEE Trans. Antennas Propag.* **1966**, *14*, 302-307.
- (73) Han, F.; Armstrong, T.; Andres-Arroyo, A.; Bennett, D.; Soeriyadi, A.; Chamazketi, A. A.; Bakthavathsalam, P.; Tilley, R. D.; Gooding, J. J.; Reece, P. J. Optical Tweezers-Based Characterisation of Gold Core–Satellite Plasmonic Nano-Assemblies Incorporating Thermo-Responsive Polymers. *Nanoscale* **2020**, *12*, 1680-1687.
- (74) Zhao, Y.; Saleh, A. A.; Van De Haar, M. A.; Baum, B.; Briggs, J. A.; Lay, A.; Reyes-Becerra, O. A.; Dionne, J. A. Nanoscopic Control and Quantification of Enantioselective Optical Forces. *Nat. Nanotechnol.* **2017**, *12*, 1055-1059.
- (75) Wong, V.; Ratner, M. A. Gradient and Nongradient Contributions to Plasmon-Enhanced Optical Forces on Silver Nanoparticles. *Phys. Rev. B* **2006**, *73*, 075416.

- (76) Wang, K.; Schonbrun, E.; Steinvurzel, P.; Crozier, K. B. Scannable Plasmonic Trapping Using a Gold Stripe. *Nano Lett.* **2010**, *10*, 3506-3511.
- (77) Timmermans, F. J.; Lenferink, A. T.; van Wolferen, H. A.; Otto, C. Correlative SEM SERS for Quantitative Analysis of Dimer Nanoparticles. *Analyst* **2016**, *141*, 6455-6462.
- (78) Li, D.-B.; Sun, X.-J.; Jia, Y.-P.; Stockman, M. I.; Paudel, H. P.; Song, H.; Jiang, H.; Li, Z.-M. Direct Observation of Localized Surface Plasmon Field Enhancement by Kelvin Probe Force Microscopy. *Light-Sci. Appl.* **2017**, *6*, e17038.
- (79) Rácz, P.; Pápa, Z.; Márton, I.; Budai, J.; Wróbel, P.; Stefaniuk, T.; Prietl, C.; Krenn, J. R.; Dombi, P. Measurement of Nanoplasmonic Field Enhancement with Ultrafast Photoemission. *Nano Lett.* **2017**, *17*, 1181-1186.
- (80) Campion, A.; Kambhampati, P. Surface-Enhanced Raman Scattering. *Chem. Soc. Rev.* **1998**, *27*, 241-250.
- (81) Lalisse, A.; Tessier, G.; Plain, J.; Baffou, G. Plasmonic Efficiencies of Nanoparticles Made of Metal Nitrides (TiN, ZrN) Compared with Gold. *Sci. Rep-UK* **2016**, *6*, 38647.
- (82) Pin, C.; Magno, G.; Ecarnot, A.; Picard, E.; Hadji, E.; Yam, V.; de Fornel, F.; Dagens, B.; Cluzel, B. Seven at One Blow: Particle Cluster Stability in a Single Plasmonic Trap on a Silicon Waveguide. *ACS Photonics* **2020**, *7*, 1942-1949.
- (83) Mokri, K.; Mozaffari, M. H. Numerical Design of a Plasmonic Nano-Tweezer for Realizing High Optical Gradient Force. *Opt. Laser Technol.* **2019**, *119*, 105620.
- (84) Lin, P. T.; Chu, H. Y.; Lu, T. W.; Lee, P. T. Trapping Particles Using Waveguide-Coupled Gold Bowtie Plasmonic Tweezers. *Lab Chip* **2014**, *14*, 4647-4652.
- (85) Tanaka, Y.; Kaneda, S.; Sasaki, K. Nanostructured Potential of Optical Trapping Using a Plasmonic Nanoblock Pair. *Nano Lett.* **2013**, *13*, 2146-2150.

- (86) Ghorbanzadeh, M.; Jones, S.; Moravvej-Farshi, M. K.; Gordon, R. Improvement of Sensing and Trapping Efficiency of Double Nanohole Apertures *via* Enhancing the Wedge Plasmon Polariton Modes with Tapered Cusps. *ACS Photonics* **2017**, *4*, 1108-1113.
- (87) Bouloumis, T. D.; Kotsifaki, D. G.; Han, X.; Chormaic, S. N.; Truong, V. G. Fast and Efficient Nanoparticle Trapping Using Plasmonic Connected Nanoring Apertures. *Nanotechnology* **2021**, *32*, 025507.
- (88) Yang, T. P.; Yossifon, G.; Yang, Y. T. Characterization of the Near-Field and Convective Transport Behavior of Micro and Nanoparticles in Nanoscale Plasmonic Optical Lattices. *Biomicrofluidics* **2016**, *10*, 034102.
- (89) Yoshikawa, T.; Tamura, M.; Tokonami, S.; Iida, T. Optical Trap-Mediated High-Sensitivity Nanohole Array Biosensors with Random Nanospikes. *J. Phys. Chem. Lett.* **2017**, *8*, 370-374.
- (90) Huang, L.; Maerkl, S. J.; Martin, O. J. F. Integration of Plasmonic Trapping in a Microfluidic Environment. *Opt. Express* **2009**, *17*, 6018-6024.
- (91) Hong, C.; Yang, S.; Ndukaife, J. C. Optofluidic Control Using Plasmonic TiN Bowtie Nanoantenna. *Opt. Mater. Express* **2019**, *9*, 953.
- (92) Tanaka, Y.; Sasaki, K. Optical Trapping through the Localized Surface Plasmon Resonance of Engineered Gold Nanoblock Pairs. *Opt. Express* **2011**, *19*, 17462.
- (93) Ploschner, M.; Mazilu, M.; Krauss, T. F.; Dholakia, K. Optical Forces near a Nanoantenna. *J. Nanophotonics* **2010**, *4*, 041570.
- (94) Wang, G.; Ying, Z.; Ho, H. P.; Huang, Y.; Zou, N.; Zhang, X. Nano-Optical Conveyor Belt with Waveguide-Coupled Excitation. *Opt. Lett.* **2016**, *41*, 528-531.

- (95) Xu, Z.; Song, W.; Crozier, K. B. Direct Particle Tracking Observation and Brownian Dynamics Simulations of a Single Nanoparticle Optically Trapped by a Plasmonic Nanoaperture. *ACS Photonics* **2018**, *5*, 2850-2859.
- (96) Hong, C.; Yang, S.; Ndukaife, J. C. Stand-Off Trapping and Manipulation of Sub-10nm Objects and Biomolecules Using Opto-Thermo-Electrohydrodynamic Tweezers. *Nat. Nanotechnol.* **2020**, *15*, 908-913.
- (97) Jiang, M.; Wang, G.; Xu, W.; Ji, W.; Zou, N.; Ho, H. P.; Zhang, X. Two-Dimensional Arbitrary Nano-Manipulation on a Plasmonic Metasurface. *Opt. Lett.* **2018**, *43*, 1602-1605.
- (98) Krishnan, A.; Huang, N.; Wu, S. H.; Martinez, L. J.; Povinelli, M. L. Enhanced and Selective Optical Trapping in a Slot-Graphite Photonic Crystal. *Opt. Express* **2016**, *24*, 23271-23279.
- (99) Ghosh, S.; Ghosh, A. Mobile Nanotweezers for Active Colloidal Manipulation. *Sci. Robot.* **2018**, *3*, eaaq0076.
- (100) Cai, H.; Poon, A. W. Optical Manipulation of Microparticles Using Whispering-Gallery Modes in a Silicon Nitride Microdisk Resonator. *Opt. Lett.* **2011**, *36*, 4257-4259.
- (101) Nan, F.; Yan, Z. Silver-Nanowire-Based Interferometric Optical Tweezers for Enhanced Optical Trapping and Binding of Nanoparticles. *Adv. Funct. Mater.* **2019**, *29*, 1808258.
- (102) Zheng, J.; Xing, X.; Yang, J.; Shi, K.; He, S. Hybrid Optofluidics and Three-Dimensional Manipulation Based on Hybrid Photothermal Waveguides. *NPG Asia Mater.* **2018**, *10*, 340-351.
- (103) Wang, K.; Crozier, K. B. Plasmonic Trapping with a Gold Nanopillar. *Chemphyschem* **2012**, *13*, 2639-2648.

- (104) Kang, J.-H.; Kim, K.; Ee, H.-S.; Lee, Y.-H.; Yoon, T.-Y.; Seo, M.-K.; Park, H.-G. Low-Power Nano-Optical Vortex Trapping *via* Plasmonic Diabolo Nanoantennas. *Nat. Commun.* **2011**, *2*, 582.
- (105) Khosravi, M. A.; Aqhili, A.; Vasini, S.; Khosravi, M. H.; Darbari, S.; Hajizadeh, F. Gold Cauldrons as Efficient Candidates for Plasmonic Tweezers. *Sci. Rep-UK* **2020**, *10*, 19356.
- (106) Hao, E.; Schatz, G. C. Electromagnetic Fields around Silver Nanoparticles and Dimers. *J. Chem. Phys.* **2004**, *120*, 357-366.
- (107) Jain, P. K.; Eustis, S.; El-Sayed, M. A. Plasmon Coupling in Nanorod Assemblies: Optical Absorption, Discrete Dipole Approximation Simulation, and Exciton-Coupling Model. *J. Phys. Chem. B* **2006**, *110*, 18243-18253.
- (108) Jain, P. K.; El-Sayed, M. A. Plasmonic Coupling in Noble Metal Nanostructures. *Chem. Phys. Lett.* **2010**, *487*, 153-164.
- (109) Griffiths, D. J. *Introduction to Electrodynamics*, 3rd ed.; Prentice Hall: New Jersey, USA, 1999; pp 58-193.
- (110) Guffey, M. J.; Scherer, N. F. All-Optical Patterning of Au Nanoparticles on Surfaces Using Optical Traps. *Nano Lett.* **2010**, *10*, 4302-4308.
- (111) Urban, A. S.; Lutich, A. A.; Stefani, F. D.; Feldmann, J. Laser Printing Single Gold Nanoparticles. *Nano Lett.* **2010**, *10*, 4794-4798.
- (112) Gargiulo, J.; Violi, I. L.; Cerrota, S.; Chvatal, L.; Cortes, E.; Perassi, E. M.; Diaz, F.; Zemanek, P.; Stefani, F. D. Accuracy and Mechanistic Details of Optical Printing of Single Au and Ag Nanoparticles. *ACS Nano* **2017**, *11*, 9678-9688.

- (113) Coronado, E. A.; Encina, E. R.; Stefani, F. D. Optical Properties of Metallic Nanoparticles: Manipulating Light, Heat and Forces at the Nanoscale. *Nanoscale* **2011**, *3*, 4042-4059.
- (114) Zaza, C.; Violi, I. L.; Gargiulo, J.; Chiarelli, G.; Schumacher, L.; Jakobi, J.; Olmos-Trigo, J.; Cortes, E.; König, M.; Barcikowski, S.; Schlücker, S.; Sáenz, J. J.; Maier, S. A.; Stefani, F. D. Size-Selective Optical Printing of Silicon Nanoparticles through Their Dipolar Magnetic Resonance. *ACS Photonics* **2019**, *6*, 815-822.
- (115) Giannini, V.; Fernandez-Dominguez, A. I.; Heck, S. C.; Maier, S. A. Plasmonic Nanoantennas: Fundamentals and Their Use in Controlling the Radiative Properties of Nanoemitters. *Chem. Rev.* **2011**, *111*, 3888-3912.
- (116) Roxworthy, B. J.; Ko, K. D.; Kumar, A.; Fung, K. H.; Chow, E. K. C.; Liu, G. L.; Fang, N. X.; Toussaint, K. C. Application of Plasmonic Bowtie Nanoantenna Arrays for Optical Trapping, Stacking, and Sorting. *Nano Lett.* **2012**, *12*, 796-801.
- (117) Jones, S.; Andrén, D.; Karpinski, P.; Käll, M. Photothermal Heating of Plasmonic Nanoantennas: Influence on Trapped Particle Dynamics and Colloid Distribution. *ACS Photonics* **2018**, *5*, 2878-2887.
- (118) Righini, M.; Ghenuche, P.; Cherukulappurath, S.; Myroshnychenko, V.; García de Abajo, F. J.; Quidant, R. Nano-Optical Trapping of Rayleigh Particles and Escherichia Coli Bacteria with Resonant Optical Antennas. *Nano Lett.* **2009**, *9*, 3387-3391.
- (119) Ren, Y.; Qi, H.; Chen, Q.; Wang, S.; Ruan, L. Localized Surface Plasmon Resonance of Nanotriangle Dimers at Different Relative Positions. *J. Quant. Spectrosc. Ra.* **2017**, *199*, 45-51.

- (120) Fu, R.; Yan, Y.; Roberts, C.; Liu, Z.; Chen, Y. The Role of Dipole Interactions in Hyperthermia Heating Colloidal Clusters of Densely-Packed Superparamagnetic Nanoparticles. *Sci. Rep-UK* **2018**, *8*, 4704.
- (121) Hong, S.; Shim, O.; Kwon, H.; Choi, Y. Autoenhanced Raman Spectroscopy via Plasmonic Trapping for Molecular Sensing. *Anal. Chem.* **2016**, *88*, 7633-7638.
- (122) Yan, B.; Thubagere, A.; Premasiri, W. R.; Ziegler, L. D.; Dal Negro, L.; Reinhard, B. M. Engineered SERS Substrates with Multiscale Signal Enhancement: Nanoparticle Cluster Arrays. *ACS Nano* **2009**, *3*, 1190-1202.
- (123) Shi, Y.; Zhao, H.; Nguyen, K. T.; Zhang, Y.; Chin, L. K.; Zhu, T.; Yu, Y.; Cai, H.; Yap, P. H.; Liu, P. Y.; Xiong, S.; Zhang, J.; Qiu, C. W.; Chan, C. T.; Liu, A. Q. Nanophotonic Array-Induced Dynamic Behavior for Label-Free Shape-Selective Bacteria Sieving. *ACS Nano* **2019**, *13*, 12070-12080.
- (124) Jain, P. K.; Huang, W.; El-Sayed, M. A. On the Universal Scaling Behavior of the Distance Decay of Plasmon Coupling in Metal Nanoparticle Pairs: A Plasmon Ruler Equation. *Nano Lett.* **2007**, *7*, 2080-2088.
- (125) Wang, H.; Chen, K.; Pan, J.; Huang, S.; Lin, J.; Xie, W.; Huang, X. Modified Plasmonic Response of Dimer Nanoantennas with Nonlocal Effects: From Near-Field Enhancement to Optical Force. *J. Quant. Spectrosc. Ra.* **2020**, *245*, 106878.
- (126) Jain, P. K.; El-Sayed, M. A. Universal Scaling of Plasmon Coupling in Metal Nanostructures: Extension from Particle Pairs to Nanoshells. *Nano Lett.* **2007**, *7*, 2854-2858.
- (127) Tabor, C.; Van, H. D.; El-Sayed, M. A. Effect of Orientation on Plasmonic Coupling between Gold Nanorods. *ACS Nano* **2009**, *3*, 3670-3678.

- (128) Tabor, C.; Murali, R.; Mahmoud, M.; El-Sayed, M. A. On the Use of Plasmonic Nanoparticle Pairs as a Plasmon Ruler: The Dependence of the Near-Field Dipole Plasmon Coupling on Nanoparticle Size and Shape. *J. Phys. Chem. A* **2009**, *113*, 1946-1953.
- (129) Jain, P. K.; El-Sayed, M. A. Surface Plasmon Coupling and Its Universal Size Scaling in Metal Nanostructures of Complex Geometry: Elongated Particle Pairs and Nanosphere Trimers. *J. Phys. Chem. C* **2008**, *112*, 4954-4960.
- (130) Chen, Q.; Ren, Y.; Qi, H.; Ruan, L. Influence of PEG Coating on Optical and Thermal Response of Gold Nanospheres and Nanorods. *J. Quant. Spectrosc. Ra.* **2018**, *212*, 1-9.
- (131) Ren, Y.; Chen, Q.; Qi, H.; Liming, R.; Dai, J. Phase Transition Induced by Localized Surface Plasmon Resonance of Nanoparticle Assemblies. *Int. J. Heat Mass Tran.* **2018**, *127*, 244-252.
- (132) Liu, Z.; Li, Q.; Zhang, W.; Yang, Y.; Qiu, M. Nanoscale Control of Temperature Distribution Using a Plasmonic Trimer. *Plasmonics* **2015**, *10*, 911-918.
- (133) Ruan, Z. H.; Li, Y. D.; Yuan, Y.; Lin, K. F.; Tan, H. P. Energy-Absorption-Based Explanation of the Photocatalytic Activity Enhancement Mechanism of TiO₂ Nanofibers. *Int. Hydrogen Energ.* **2019**, *44*, 21569-21576.
- (134) Yoo, D.; Gurunatha, K. L.; Choi, H. K.; Mohr, D. A.; Ertsgaard, C. T.; Gordon, R.; Oh, S. H. Low-Power Optical Trapping of Nanoparticles and Proteins with Resonant Coaxial Nanoaperture Using 10nm Gap. *Nano Lett.* **2018**, *18*, 3637-3642.
- (135) Verschueren, D.; Shi, X.; Dekker, C. Nano-Optical Tweezing of Single Proteins in Plasmonic Nanopores. *Small Methods* **2019**, *3*, 1800465.
- (136) Sinton, D.; Gordon, R.; Brolo, A. G. Nanohole Arrays in Metal Films as Optofluidic Elements: Progress and Potential. *Microfluid. Nanofluid.* **2008**, *4*, 107-116.

- (137) Han, X.; Truong, V. G.; Thomas, P. S.; Chormaic, S. N. Sequential Trapping of Single Nanoparticles Using a Gold Plasmonic Nanohole Array. *Photonics Res.* **2018**, *6*, 984-986.
- (138) Wu, W.; Ruan, Z.; Li, J.; Li, Y.; Jiang, Y.; Xu, X.; Li, D.; Yuan, Y.; Lin, K. *In Situ* Preparation and Analysis of Bimetal Co-Doped Mesoporous Graphitic Carbon Nitride with Enhanced Photocatalytic Activity. *Nano-Micro Letters* **2019**, *11*, 10.
- (139) Tu, L.; Li, X.; Bian, S.; Yu, Y.; Li, J.; Huang, L.; Liu, P.; Wu, Q.; Wang, W. Label-Free and Real-Time Monitoring of Single Cell Attachment on Template-Stripped Plasmonic Nano-Holes. *Sci. Rep-UK* **2017**, *7*, 11020.
- (140) Ghosh, S.; Ghosh, A. Photothermal Effects in Mobile Nanotweezers. Proceedings of 2018 4th IEEE International Conference on Emerging Electronics (ICEE), Bengaluru, India, 17-19 Dec. 2018; IEEE: Bengaluru, India, 2019; pp 1-4.
- (141) Ghosh, S.; Ghosh, A. Design Considerations for Effective Thermal Management in Mobile Nanotweezers. *J. Micro-Bio Robot.* **2020**, *16*, 33-42.
- (142) Dasgupta, D.; Pally, D.; Saini, D. K.; Bhat, R.; Ghosh, A. Nanomotors Sense Local Physicochemical Heterogeneities in Tumor Microenvironments. *Angew. Chem. Int. Edit.* **2020**, *59*, 23690-23696.
- (143) Wu, Y.; Fu, A.; Yossifon, G. Active Particle Based Selective Transport and Release of Cell Organelles and Mechanical Probing of a Single Nucleus. *Small* **2020**, *16*, 1906682.
- (144) Toshimitsu, M.; Matsumura, Y.; Shoji, T.; Kitamura, N.; Takase, M.; Murakoshi, K.; Yamauchi, H.; Ito, S.; Miyasaka, H.; Nobuhiro, A. Metallic-Nanostructure-Enhanced Optical Trapping of Flexible Polymer Chains in Aqueous Solution as Revealed by Confocal Fluorescence Microspectroscopy. *J. Phys. Chem. C* **2012**, *116*, 14610-14618.

- (145) Samadi, M.; Darbari, S.; Moravvej-Farshi, M. K. Numerical Investigation of Tunable Plasmonic Tweezers Based on Graphene Stripes. *Sci. Rep-UK* **2017**, *7*, 14533.
- (146) Xu, L.; Mou, F.; Gong, H.; Luo, M.; Guan, J. Light-Driven Micro/Nanomotors: From Fundamentals to Applications. *Chem. Soc. Rev.* **2017**, *46*, 6905-6926.
- (147) Wong, H. M. K.; Righini, M.; Gates, J. C.; Smith, P. G. R.; Pruneri, V.; Quidant, R. On-a-Chip Surface Plasmon Tweezers. *Appl. Phys. Lett.* **2011**, *99*, 061107.
- (148) Zhu, X.; Cicek, A.; Li, Y.; Yanik, A. A. Plasmofluidic Microlenses for Label-Free Optical Sorting of Exosomes. *Sci. Rep-UK* **2019**, *9*, 8593.
- (149) Ma, B.; Yao, B.; Peng, F.; Yan, S.; Lei, M.; Rupp, R. Optical Sorting of Particles by Dual-Channel Line Optical Tweezers. *J. Optics-UK* **2012**, *14*, 105702.
- (150) Ndukaife, J. C.; Kildishev, A. V.; Nnanna, A. G.; Shalaev, V. M.; Wereley, S. T.; Boltasseva, A. Long-Range and Rapid Transport of Individual Nano-Objects by a Hybrid Electrothermoplasmonic Nanotweezer. *Nat. Nanotechnol.* **2016**, *11*, 53-59.
- (151) Ndukaife, J. C.; Xuan, Y.; Nnanna, A. G. A.; Kildishev, A. V.; Shalaev, V. M.; Wereley, S. T.; Boltasseva, A. High-Resolution Large-Ensemble Nanoparticle Trapping with Multifunctional Thermoplasmonic Nanohole Metasurface. *ACS Nano* **2018**, *12*, 5376-5384.
- (152) Kawata, S.; Sugiura, T. Movement of Micrometer-Sized Particles in the Evanescent Field of a Laser Beam. *Opt. Lett.* **1992**, *17*, 772-774.
- (153) Quidant, R.; Girard, C. Surface-Plasmon-Based Optical Manipulation. *Laser Photonics Rev.* **2008**, *2*, 47-57.
- (154) Kawata, S.; Tani, T. Optically Driven Mie Particles in an Evanescent Field Along a Channeled Waveguide. *Opt. Lett.* **1996**, *21*, 1768-1770.

- (155) Helleso, O. G.; Lovhaugen, P.; Subramanian, A. Z.; Wilkinson, J. S.; Ahluwalia, B. S. Surface Transport and Stable Trapping of Particles and Cells by an Optical Waveguide Loop. *Lab Chip* **2012**, *12*, 3436-40.
- (156) Buchberger, A.; Maierhofer, P.; Baumgart, M.; Kraft, J.; Bergmann, A. Integrated Evanescent Field Detector for Ultrafine Particles-Theory and Concept. *Opt. Express* **2020**, *28*, 20177-20190.
- (157) Daly, M.; Sergides, M.; Nic Chormaic, S. Optical Trapping and Manipulation of Micrometer and Submicrometer Particles. *Laser Photonics Rev.* **2015**, *9*, 309-329.
- (158) Schmidt, B. S.; Yang, A. H. J.; Erickson, D.; Lipson, M. Optofluidic Trapping and Transport on Solid Core Waveguides within a Microfluidic Device. *Opt. Express* **2007**, *15*, 14322-14334.
- (159) Yang, A. H. J.; Moore, S. D.; Schmidt, B. S.; Klug, M.; Lipson, M.; Erickson, D. Optical Manipulation of Nanoparticles and Biomolecules in Sub-Wavelength Slot Waveguides. *Nature* **2009**, *457*, 71-75.
- (160) Ng, L. N.; Zervas, M. N.; Wilkinson, J. S.; Luff, B. J. Manipulation of Colloidal Gold Nanoparticles in the Evanescent Field of a Channel Waveguide. *Appl. Phys. Lett.* **2000**, *76*, 1993-1995.
- (161) Gaugiran, S.; Gétin, S.; Fedeli, J. M.; Colas, G.; Fuchs, A.; Chatelain, F.; Dérouard, J. Optical Manipulation of Microparticles and Cells on Silicon Nitride Waveguides. *Opt. Express* **2005**, *13*, 6956-6963.
- (162) Righini, M.; Girard, C.; Quidant, R. Light-Induced Manipulation with Surface Plasmons. *J. Opt. A-Pure Appl. Op.* **2008**, *10*, 093001.

- (163) Xu, X.; Dong, Y.; Wang, G.; Jiao, W.; Ying, Z.; Ho, H.-P.; Zhang, X. Reconfigurable Sorting of Nanoparticles on a Thermal Tuning Silicon Based Optofluidic Chip. *IEEE Photonics J.* **2017**, *10*, 4900107.
- (164) An, R.; Wang, G.; Ji, W.; Jiao, W.; Jiang, M.; Chang, Y.; Xu, X.; Zou, N.; Zhang, X. Controllable Trapping and Releasing of Nanoparticles by a Standing Wave on Optical Waveguides. *Opt. Lett.* **2018**, *43*, 3901-3904.
- (165) Jiao, W.; Wang, G.; Ying, Z.; Kang, Z.; Sun, T.; Zou, N.; Ho, H.-p.; Zhang, X. Optofluidic Switching of Nanoparticles Based on a WDM Tree Splitter. *IEEE Photonics J.* **2016**, *8*, 7803010.
- (166) Jiao, W.; Wang, G.; Ying, Z.; Zou, Y.; Ho, H. P.; Sun, T.; Huang, Y.; Zhang, X. Switching of Nanoparticles in Large-Scale Hybrid Electro-Optofluidics Integration. *Opt. Lett.* **2016**, *41*, 2652-2655.
- (167) Applegate Jr., R. W.; Squier, J.; Vestad, T.; Oakey, J.; Marr, D. W.; Bado, P.; Dugan, M. A.; Said, A. A. Microfluidic Sorting System Based on Optical Waveguide Integration and Diode Laser Bar Trapping. *Lab Chip* **2006**, *6*, 422-426.
- (168) Kim, J.; Shin, J. H. Stable, Free-Space Optical Trapping and Manipulation of Sub-Micron Particles in an Integrated Microfluidic Chip. *Sci. Rep-UK* **2016**, *6*, 33842.
- (169) Baker, J. E.; Sriram, R.; Miller, B. L. Recognition-Mediated Particle Detection under Microfluidic Flow with Waveguide-Coupled 2D Photonic Crystals: Towards Integrated Photonic Virus Detectors. *Lab Chip* **2017**, *17*, 1570-1577.
- (170) Renault, C.; Cluzel, B.; Dellinger, J.; Lalouat, L.; Picard, E.; Peyrade, D.; Hadji, E.; de Fornel, F. On Chip Shapeable Optical Tweezers. *Sci. Rep-UK* **2013**, *3*, 2290.

- (171) Jiang, M.; Wang, G.; Jiao, W.; Ying, Z.; Zou, N.; Ho, H.-p.; Sun, T.; Zhang, X. Plasmonic Non-Concentric Nanorings Array as an Unidirectional Nano-Optical Conveyor Belt Actuated by Polarization Rotation. *Opt. Lett.* **2017**, *42*, 259-262.
- (172) Hansen, P.; Zheng, Y.; Ryan, J.; Hesselink, L. Nano-Optical Conveyor Belt, Part I: Theory. *Nano Lett.* **2014**, *14*, 2965-2970.
- (173) Zheng, Y.; Ryan, J.; Hansen, P.; Cheng, Y. T.; Lu, T. J.; Hesselink, L. Nano-Optical Conveyor Belt, Part II: Demonstration of Handoff between Near-Field Optical Traps. *Nano Lett.* **2014**, *14*, 2971-2976.
- (174) Tanaka, Y. Y.; Albella, P.; Rahmani, M.; Giannini, V.; Maier, S. A.; Shimura, T. Plasmonic Linear Nanomotor Using Lateral Optical Forces. *Sci. Adv.* **2020**, *6*, eabc3726.
- (175) Kang, Z.; Lu, H.; Chen, J.; Chen, K.; Xu, F.; Ho, H. P. Plasmonic Graded Nano-Disks as Nano-Optical Conveyor Belt. *Opt. Express* **2014**, *22*, 19567-19572.
- (176) Miró, M.; Hansen, E. H. Miniaturization of Environmental Chemical Assays in Flowing Systems: The Lab-on-a-Valve Approach Vis-a-Vis Lab-on-a-Chip Microfluidic Devices. *Anal. Chim. Acta* **2007**, *600*, 46-57.
- (177) Zhao, H.; Chin, L. K.; Shi, Y.; Liu, P. Y.; Zhang, Y.; Cai, H.; Yap, E. P. H.; Ser, W.; Liu, A.-Q. Continuous Optical Sorting of Nanoscale Biomolecules in Integrated Microfluidic-Nanophotonic Chips. *Sensor. Actuat. B-Chem.* **2021**, *331*, 129428.
- (178) Imasaka, T.; Kawabata, Y.; Kaneta, T.; Ishidzu, Y. Optical Chromatography. *Anal. Chem.* **1995**, *67*, 1763-1765.
- (179) Kaneta, T.; Ishidzu, Y.; Mishima, N.; Imasaka, T. Theory of Optical Chromatography. *Anal. Chem.* **1997**, *69*, 2701-2710.

- (180) Hart, S. J.; Terray, A. V. Refractive-Index-Driven Separation of Colloidal Polymer Particles Using Optical Chromatography. *Appl. Phys. Lett.* **2003**, *83*, 5316-5318.
- (181) Zhu, X.; Cicek, A.; Li, Y.; Yanik, A. A. Optofluidic Chromatography: Label-Free Sorting of Exosomes with Plasmonic Microlenses. Proceedings of SPIE Nanoscience + Engineering, California, USA, 11-15 Aug. 2019; SPIE: Washington, USA, 2019; pp 1108339.
- (182) Righini, M.; Zelenina, A. S.; Girard, C.; Quidant, R. Parallel and Selective Trapping in a Patterned Plasmonic Landscape. *Nat. Phys.* **2007**, *3*, 477-480.
- (183) Wang, K.; Schonbrun, E.; Steinvurzel, P.; Crozier, K. B. Trapping and Rotating Nanoparticles Using a Plasmonic Nano-Tweezer with an Integrated Heat Sink. *Nat. Commun.* **2011**, *2*, 1-6.
- (184) Garcia-Guirado, J.; Rica, R. I. A.; Ortega, J.; Medina, J.; Sanz, V.; Ruiz-Reina, E.; Quidant, R. Overcoming Diffusion-Limited Biosensing by Electrothermoplasmonics. *ACS Photonics* **2018**, *5*, 3673-3679.
- (185) Lin, L.; Wang, M.; Peng, X.; Lissek, E. N.; Mao, Z.; Scarabelli, L.; Adkins, E.; Coskun, S.; Unalan, H. E.; Korgel, B. A.; Liz-Marzán, L. M.; Florin, E.-L.; Zheng, Y. Opto-Thermoelectric Nanotweezers. *Nat. Photonics* **2018**, *12*, 195-201.
- (186) Pughazhendi, A.; Chen, Z.; Wu, Z.; Li, J.; Zheng, Y. Opto-Thermoelectric Tweezers: Principles and Applications. *Front. Phys.-Lausanne* **2020**, *8*, 580014.
- (187) Braun, M.; Cichos, F. Optically Controlled Thermophoretic Trapping of Single Nano-Objects. *ACS Nano* **2013**, *7*, 11200-11208.
- (188) Fischer, P.; Ghosh, A. Magnetically Actuated Propulsion at Low Reynolds Numbers: Towards Nanoscale Control. *Nanoscale* **2011**, *3*, 557-563.

- (189) Garcia-Gradilla, V.; Orozco, J.; Sattayasamitsathit, S.; Soto, F.; Kuralay, F.; Pourazary, A.; Katzenberg, A.; Gao, W.; Shen, Y.; Wang, J. Functionalized Ultrasound-Propelled Magnetically Guided Nanomotors: Toward Practical Biomedical Applications. *ACS Nano* **2013**, *7*, 9232-9240.
- (190) Shamay, Y.; Adar, L.; Ashkenasy, G.; David, A. Light Induced Drug Delivery into Cancer Cells. *Biomaterials* **2011**, *32*, 1377-1386.
- (191) Meerovich, I.; Nichols, M. G.; Dash, A. K. Low-Intensity Light-Induced Drug Release from a Dual Delivery System Comprising of a Drug Loaded Liposome and a Photosensitive Conjugate. *J. Drug Target.* **2020**, *28*, 655-667.
- (192) Hacohen, N.; Ip, C. J.; Gordon, R. Analysis of Egg White Protein Composition with Double Nanohole Optical Tweezers. *ACS Omega* **2018**, *3*, 5266-5272.
- (193) Li, Y.; Liu, X.; Li, B. Single-Cell Biomagnifier for Optical Nanoscopes and Nanotweezers. *Light-Sci. Appl.* **2019**, *8*, 61.
- (194) Shoji, T.; Tsuboi, Y. Plasmonic Optical Tweezers toward Molecular Manipulation: Tailoring Plasmonic Nanostructure, Light Source, and Resonant Trapping. *J. Phys. Chem. Lett.* **2014**, *5*, 2957-2967.
- (195) Yanik, A. A.; Huang, M.; Kamohara, O.; Artar, A.; Geisbert, T. W.; Connor, J. H.; Altug, H. An Optofluidic Nanoplasmonic Biosensor for Direct Detection of Live Viruses from Biological Media. *Nano Lett.* **2010**, *10*, 4962-4969.
- (196) Ueno, K.; Misawa, H. Surface Plasmon-Enhanced Photochemical Reactions. *J. Photoch. Photobio. C* **2013**, *15*, 31-52.
- (197) Saylan, Y.; Akgönüllü, S.; Denizli, A. Plasmonic Sensors for Monitoring Biological and Chemical Threat Agents. *Biosensors* **2020**, *10*, 142.

- (198) Nie, S.; Emory, S. R. Probing Single Molecules and Single Nanoparticles by Surface-Enhanced Raman Scattering. *Science* **1997**, *275*, 1102-1106.
- (199) Blackie, E. J.; Le Ru, E. C.; Etchegoin, P. G. Single-Molecule Surface-Enhanced Raman Spectroscopy of Nonresonant Molecules. *J. Am. Chem. Soc.* **2009**, *131*, 14466-14472.
- (200) Koya, A. N.; Cunha, J.; Guo, T. L.; Toma, A.; Garoli, D.; Wang, T.; Juodkazis, S.; Cojoc, D.; Proietti Zaccaria, R. Novel Plasmonic Nanocavities for Optical Trapping-Assisted Biosensing Applications. *Adv. Opt. Mater.* **2020**, *8*, 1901481.
- (201) Yuan, Y.; Lin, Y.; Gu, B.; Panwar, N.; Tjin, S. C.; Song, J.; Qu, J.; Yong, K.-T. Optical Trapping-Assisted SERS Platform for Chemical and Biosensing Applications: Design Perspectives. *Coordin. Chem. Rev.* **2017**, *339*, 138-152.
- (202) Burkhartsmeier, J.; Wang, Y.; Wong, K. S.; Gordon, R. Optical Trapping, Sizing, and Probing Acoustic Modes of a Small Virus. *Appl. Sci-Basel* **2020**, *10*, 394.
- (203) Komoto, S.; Nagai, T.; Takao, R.; Ushiro, K.; Matsumoto, M.; Shoji, T.; Linklater, D. P.; Juodkazis, S.; Tsuboi, Y. Optical Trapping of Polystyrene Nanoparticles on Black Silicon: Implications for Trapping and Studying Bacteria and Viruses. *ACS Appl. Nano Mater.* **2020**, *3*, 9831-9841.
- (204) Bar-On, Y. M.; Flamholz, A.; Phillips, R.; Milo, R. SARS-CoV-2 (Covid-19) by the Numbers. *Elife* **2020**, *9*, e57309.
- (205) Lin, L.; Peng, X.; Wang, M.; Scarabelli, L.; Mao, Z.; Liz-Marzán, L. M.; Becker, M. F.; Zheng, Y. Light-Directed Reversible Assembly of Plasmonic Nanoparticles Using Plasmon-Enhanced Thermophoresis. *ACS Nano* **2016**, *10*, 9659-9668.
- (206) Shen, Y.; Yalikul, Y.; Tanaka, Y. Recent Advances in Microfluidic Cell Sorting Systems. *Sensor. Actuat. B-Chem.* **2019**, *282*, 268-281.

- (207) Haverty, P. M.; Lin, E.; Tan, J.; Yu, Y.; Lam, B.; Lianoglou, S.; Neve, R. M.; Martin, S.; Settleman, J.; Yauch, R. L. Reproducible Pharmacogenomic Profiling of Cancer Cell Line Panels. *Nature* **2016**, *533*, 333-337.
- (208) Cossarizza, A.; Chang, H. D.; Radbruch, A.; Acs, A.; Adam, D.; Adam-Klages, S.; Agace, W. W.; Aghaepour, N.; Akdis, M.; Allez, M. Guidelines for the Use of Flow Cytometry and Cell Sorting in Immunological Studies. *Eur. J. Immunol.* **2019**, *49*, 1457-1973.
- (209) Mazutis, L.; Gilbert, J.; Ung, W. L.; Weitz, D. A.; Griffiths, A. D.; Heyman, J. A. Single-Cell Analysis and Sorting Using Droplet-Based Microfluidics. *Nat. Protoc.* **2013**, *8*, 870-891.
- (210) Hulett, H. R.; Bonner, W. A.; Barrett, J.; Herzenberg, L. A. Cell Sorting: Automated Separation of Mammalian Cells as a Function of Intracellular Fluorescence. *Science* **1969**, *166*, 747-749.
- (211) Franke, T.; Braunmüller, S.; Schmid, L.; Wixforth, A.; Weitz, D. Surface Acoustic Wave Actuated Cell Sorting (SAWACS). *Lab Chip* **2010**, *10*, 789-794.
- (212) Shields IV, C. W.; Ohiri, K. A.; Szott, L. M.; López, G. P. Translating Microfluidics: Cell Separation Technologies and Their Barriers to Commercialization. *Cytom. Part B-Clin. Cy.* **2017**, *92*, 115-125.
- (213) Sahu, S. P.; Mahigir, A.; Chidester, B.; Veronis, G.; Gartia, M. R. Ultrasensitive Three-Dimensional Orientation Imaging of Single Molecules on Plasmonic Nanohole Arrays Using Second Harmonic Generation. *Nano Lett.* **2019**, *19*, 6192-6202.
- (214) Vicidomini, G.; Bianchini, P.; Diaspro, A. STED Super-Resolved Microscopy. *Nat. Methods* **2018**, *15*, 173-182.

- (215) Betzig, E.; Patterson, G. H.; Sougrat, R.; Lindwasser, O. W.; Olenych, S.; Bonifacino, J. S.; Davidson, M. W.; Lippincott-Schwartz, J.; Hess, H. F. Imaging Intracellular Fluorescent Proteins at Nanometer Resolution. *Science* **2006**, *313*, 1642-1645.
- (216) Rust, M. J.; Bates, M.; Zhuang, X. Sub-Diffraction-Limit Imaging by Stochastic Optical Reconstruction Microscopy (STORM). *Nat. Methods* **2006**, *3*, 793-796.
- (217) Vegh, R. B.; Bravaya, K. B.; Bloch, D. A.; Bommarius, A. S.; Tolbert, L. M.; Verkhovsky, M.; Krylov, A. I.; Solntsev, K. M. Chromophore Photoreduction in Red Fluorescent Proteins Is Responsible for Bleaching and Phototoxicity. *J. Phys. Chem. B* **2014**, *118*, 4527-4534.
- (218) Qi, X.; Liu, H.; Guo, W.; Lin, W.; Lin, B.; Jin, Y.; Deng, X. New Opportunities: Second Harmonic Generation of Boron-Doped Graphene Quantum Dots for Stem Cells Imaging and Ultraprecise Tracking in Wound Healing. *Adv. Funct. Mater.* **2019**, *29*, 1902235.
- (219) Spreyer, F.; Zhao, R.; Huang, L.; Zentgraf, T. Second Harmonic Imaging of Plasmonic Pancharatnam-Berry Phase Metasurfaces Coupled to Monolayers of WS₂. *Nanophotonics* **2020**, *9*, 351-360.
- (220) Metzger, B.; Hentschel, M.; Giessen, H. Probing the Near-Field of Second-Harmonic Light around Plasmonic Nanoantennas. *Nano Lett.* **2017**, *17*, 1931-1937.
- (221) Yang, K.-Y.; Butet, J. r. m.; Yan, C.; Bernasconi, G. D.; Martin, O. J. Enhancement Mechanisms of the Second Harmonic Generation from Double Resonant Aluminum Nanostructures. *ACS Photonics* **2017**, *4*, 1522-1530.
- (222) Eigler, D. M.; Schweizer, E. K. Positioning Single Atoms with a Scanning Tunnelling Microscope. *Nature* **1990**, *344*, 524-526.

- (223) Schuler, B.; Fatayer, S.; Mohn, F.; Moll, N.; Pavliček, N.; Meyer, G.; Peña, D.; Gross, L. Reversible Bergman Cyclization by Atomic Manipulation. *Nat. Chem.* **2016**, *8*, 220-224.
- (224) Pavliček, N.; Gawel, P.; Kohn, D. R.; Majzik, Z.; Xiong, Y.; Meyer, G.; Anderson, H. L.; Gross, L. Polyynes Formation *via* Skeletal Rearrangement Induced by Atomic Manipulation. *Nat. Chem.* **2018**, *10*, 853-858.
- (225) Sloan, P. A.; Palmer, R. Two-Electron Dissociation of Single Molecules by Atomic Manipulation at Room Temperature. *Nature* **2005**, *434*, 367-371.
- (226) Stehle, C.; Bender, H.; Zimmermann, C.; Kern, D.; Fleischer, M.; Slama, S. Plasmonically Tailored Micropotentials for Ultracold Atoms. *Nat. Photonics* **2011**, *5*, 494-498.
- (227) Mildner, M.; Horrer, A.; Fleischer, M.; Zimmermann, C.; Slama, S. Plasmonic Trapping Potentials for Cold Atoms. *J. Phys. B-At. Mol. Opt. Phys.* **2018**, *51*, 135005.
- (228) Xuan, M.; Mestre, R.; Gao, C.; Zhou, C.; He, Q.; Sanchez, S. Noncontinuous Super-Diffusive Dynamics of a Light-Activated Nanobottle Motor. *Angew. Chem. Int. Edit.* **2018**, *57*, 6838-6842.
- (229) Zhou, D.; Zhuang, R.; Chang, X.; Li, L. Enhanced Light-Harvesting Efficiency and Adaptation: A Review on Visible-Light-Driven Micro/Nanomotors. *Research* **2020**, *2020*, 6821595.
- (230) Yang, J.; Zhang, C.; Wang, X.; Wang, W.; Xi, N.; Liu, L. Development of Micro- and Nanorobotics: A Review. *Sci. China Technol. Sc.* **2019**, *62*, 1.
- (231) Roxworthy, B. J.; Bhuiya, A. M.; Vanka, S. P.; Toussaint Jr., K. C. Understanding and Controlling Plasmon-Induced Convection. *Nat. Commun.* **2014**, *5*, 3173.

(232) Gargiulo, J.; Brick, T.; Violi, I. L.; Herrera, F. C.; Shibanuma, T.; Albella, P.; Requejo, F. G.; Cortes, E.; Maier, S. A.; Stefani, F. D. Understanding and Reducing Photothermal Forces for the Fabrication of Au Nanoparticle Dimers by Optical Printing. *Nano Lett.* **2017**, *17*, 5747-5755.